

A Class of Parameterized Loss Functions for Classification: Optimization Tradeoffs and Robustness Characteristics

Tyler Sypherd*, Mario Diaz†, Harshit Laddha*,
Lalitha Sankar*, Peter Kairouz‡, Gautam Dasarathy*

*Arizona State University, {tsypherd,hladdha,lsankar,gautamd}@asu.edu

† Centro de Investigación en Matemáticas A.C., diaztorres@imat.mx

‡ Google AI, kairouz@google.com

Abstract

We introduce a parameterized class of loss functions called α -loss, $\alpha \in (0, \infty]$, to the setting of classification. This family, which includes the log-loss ($\alpha = 1$) and the 0-1 loss ($\alpha = \infty$) as special cases, comes with compelling properties which enables the practitioner to choose among a host of operating conditions that are important in modern machine learning tasks. We study α -loss theoretically with the local-quasi-convexity of the optimization landscape and provide new results in this area. Practically, we perform class imbalance, robustness, and classification experiments on benchmark datasets. Our main conclusion is that log-loss ($\alpha = 1$) is not special; certain tasks may favor different regimes of α .

1 Introduction

The performance of a classification algorithm, in terms of accuracy, tractability, and convergence guarantees depends crucially on the choice of the loss function. Consider a feature vector $X \in \mathcal{X}$, an unknown finite-valued label $Y \in \mathcal{Y}$, and a hypothesis $h : \mathcal{X} \rightarrow \mathcal{Y}$. The canonical 0-1 loss, given by $\mathbb{1}[h(X) \neq Y]$, is considered an ideal loss function that captures the probability of incorrectly guessing the true label Y using $h(X)$. However, since the 0-1 loss is neither continuous nor differentiable, its applicability in state-of-the-art learning algorithms is highly restricted. As a result, there has been much interest in identifying surrogate loss functions that approximate the 0-1 loss [1–6]. Common surrogate loss functions include log-loss, squared loss, and hinge loss. However, as classification is applied to broader contexts including scenarios where data may be noisy (e.g., incorrect labels) or have imbalanced classes (e.g., very few samples capturing anomalous events that are crucial to detect), there is a need for good surrogate loss functions that are also robust to these practical challenges.

We propose to address these challenges via a recently introduced class of loss functions, α -loss. This class was originally conceived in a privacy setting in [7] by Liao *et al.* who introduced α -loss, parameterized by $\alpha \in [1, \infty]$, to quantify information leakage for a class of adversarial threat models. The viability of α -loss as a possible family of surrogate loss functions for binary classification was suggested in [6]. Focusing on the classification context, we present α -loss for $\alpha \in (0, \infty]$ and establish how the parameter α enables the practitioner to choose among a host of operating conditions that are important in modern machine learning tasks.

This work is supported in part by the NSF under grants CIF-1815361 and CIF-1901243.

Our Contributions: Our main contribution is a family of loss functions that, in addition to including the oft-used log-loss and highly desirable 0-1 loss, captures the inherent trade-offs between classification accuracy, convexity of the optimization landscape, and robustness to noise and outliers. We provide both theoretical and experimental evidence for these trade-offs as summarized below:

- (1) We show that the margin-based form of α -loss is classification-calibrated over the entire range of α . Further, we prove that the margin-based α -loss is convex for $0 < \alpha \leq 1$ and quasi-convex for $\alpha > 1$. In the context of logistic regression, we exploit this margin-based form and its Lipschitz property to obtain generalization results using Rademacher complexity.
- (2) For logistic regression, we show that the true risk is Strictly-Locally-Quasi-Convex (SLQC) (as defined by Hazan *et al.* in [8]) for all α . Furthermore, we provide bounds on the degradation of the SLQC parameters as α increases, thereby highlighting the effect of quasi-convexity (for $\alpha > 1$). More broadly, we present a lemma that introduces an equivalent condition for the direction of descent in the definition of SLQC; this can be of independent interest.
- (3) For logistic regression, we also provide a uniform generalization result for every $\alpha \in [1, \infty]$. We show that with increasing α , the empirical α -risk more closely resembles the probability of error for every hypothesis. To this end, we highlight the saturation effect of α -loss. We find that one does not need to search too far in the range of α . Indeed, in experiments we find that the accuracy-maximizing $\alpha^* \in [.8, 4]$.
- (4) Finally, we illustrate our results using well-studied datasets such as MNIST, Fashion MNIST and CIFAR-10 and neural networks including one and two layer CNNs. We explore three contexts to compare the accuracy of α -loss against that of log-loss: original datasets, noisy datasets (with a fraction of labels flipped or pixels perturbed), and class imbalanced datasets (reduced samples in specific classes of above mentioned datasets). In particular, in the noisy labels and imbalanced class settings, we show that tuning α away from $\alpha = 1$ (log-loss) can enhance both accuracy and robustness.

1.1 Related Work

Surrogate loss functions for the 0-1 loss have been widely of interest to the machine learning and statistics communities [1–4, 9–14]. Recently, there has been renewed interest in alternative losses for classification [7, 10, 11, 14, 15] other than the oft-used log-loss. While early research was predominantly focused on convex losses [1, 3, 4, 9], more recent works propose the use of non-convex losses as a means to moderate the behavior of an algorithm [2, 6, 10, 11]. In particular, motivated by superior robustness and classification accuracy of non-convex losses, Mei *et al.* in [10] study the empirical landscape of such functions. Along these lines, Hazan *et al.* [8] introduce SLQC as a means to study the unimodality of quasi-convex functions and their optimization characteristics. For SLQC functions, they provide convergence guarantees for the Normalized Gradient Descent (NGD) algorithm first introduced by Nesterov [16]. Using their methodology, we consider α -loss under logistic regression for binary classification and derive intuition about the operating characteristics of α -loss with respect to different regimes of α .

Our work is similar to [11], wherein Nguyen *et al.* present a tunable sigmoid loss which can be made arbitrarily close to the 0-1 loss. In essence, their loss moves from a smooth to non-smooth loss. Our loss is always smooth and tunes from convex to quasi-convex. We find that in the setting of deep neural networks, some quasi-convexity of the α -loss smoothes the empirical landscape. In particular, we provide strong experimental evidence for a narrow range of α to be used in practice (a limit on the amount of convexity and quasi-convexity of the loss), which significantly reduces the range of hyperparameter tuning induced by α -loss. Increasing the degree of convexity of the optimization landscape is conducive to faster optimization. Hence, our approach could serve as an alternative to other approaches whose objective is to accelerate

the optimization process, e.g., the activation function tuning in [17–19] and references therein.

From the outset, we note that in our uniform generalization guarantee of α -loss in logistic regression, we make no distributional assumptions such as those by Tsybakov, *et. al* in [20], where they assume the posterior satisfies the *margin* condition. Under such assumptions, we observe that fast rates could be achieved, but do not consider such methodologies in this work.

2 α -loss and Binary Classification

We begin by generalizing the definition of α -loss, introduced by Liao *et al.* [7], to the entire range $\alpha \in (0, \infty]$.

Definition 1. Let $\mathcal{P}(\mathcal{Y})$ be the set of probability distributions over \mathcal{Y} . For $\alpha \in (0, \infty]$, we define α -loss for $\alpha \in (0, 1) \cup (1, \infty)$, $l^\alpha : \mathcal{Y} \times \mathcal{P}(\mathcal{Y}) \rightarrow \mathbb{R}_+$ as

$$l^\alpha(y, P_Y) := \frac{\alpha}{\alpha - 1} [1 - P_Y(y)^{1-1/\alpha}], \quad (1)$$

and, by continuous extension, $l^1(y, P_Y) := -\log P_Y(y)$ and $l^\infty(y, P_Y) := 1 - P_Y(y)$.

The above definition of α -loss presents a class of loss functions that values the probabilistic estimate of the label differently for different α . For $\alpha = \infty$, minimizing the corresponding risk leads to making a single guess on the most likely label; on the other hand, for $\alpha = 1$, such a risk minimization involves minimizing the average log loss, and therefore, refining a posterior belief over all y for a given observation x . As α increases from 1 to ∞ , the loss function increasingly limits the effect of the low probability outcomes; on the other hand, as α decreases from 1 towards 0, the loss function places increasingly higher weights on the low probability outcomes until at $\alpha = 0$, by continuous extension of (1), we have $l^0(y, P_Y) = \infty$, i.e., the loss function pays an infinite cost by ignoring the training data distribution completely. This characteristic property of α -loss is highlighted in Figure 1(a) for a binomial random variable Y generated by a fair coin over 20 flips. Note that α quantifies the level of certainty placed on the posterior distribution. Thus, larger α indicate increasing certainty over a smaller set of Y while smaller α distributes the uncertainty over more (and eventually, all) possible values of Y . Indeed, for $\alpha = \infty$, the distribution becomes the hard-decoding MAP rule.

Suppose that the feature-label variable pair $(X, Y) \sim P_{X,Y}$. Observing X , the goal in classification is to construct an estimate \hat{Y} of Y . Upon inspecting (1), one may observe that the expected α -loss $\mathbb{E}_{X,Y}[l^\alpha(Y, P_{\hat{Y}|X})]$, henceforth referred to as α -risk, quantifies the effectiveness of the estimated posterior $P_{\hat{Y}|X}$. The following proposition provides an explicit characterization of the optimal risk-minimizing posterior under α -loss.

Proposition 1 ([7, Lemma 1]). For each $\alpha \in (0, \infty]$, the minimal α -risk is

$$\min_{P_{\hat{Y}|X}} \mathbb{E}_{X,Y}[l^\alpha(Y, P_{\hat{Y}|X})] = \frac{\alpha}{\alpha - 1} \left(1 - e^{-\frac{1-\alpha}{\alpha} H_\alpha^A(Y|X)} \right). \quad (2)$$

where $H_\alpha^A(Y|X) = \frac{\alpha}{1-\alpha} \log \sum_y \left(\sum_x P_{X,Y}(x, y)^\alpha \right)^{1/\alpha}$ is the Arimoto conditional entropy of order α [21]. The resulting unique minimizer, $P_{\hat{Y}|X}^*(y|x)$, is the α -tilted true posterior

$$P_{\hat{Y}|X}^*(y|x) = \frac{P_{Y|X}(y|x)^\alpha}{\sum_y P_{Y|X}(y|x)^\alpha}. \quad (3)$$

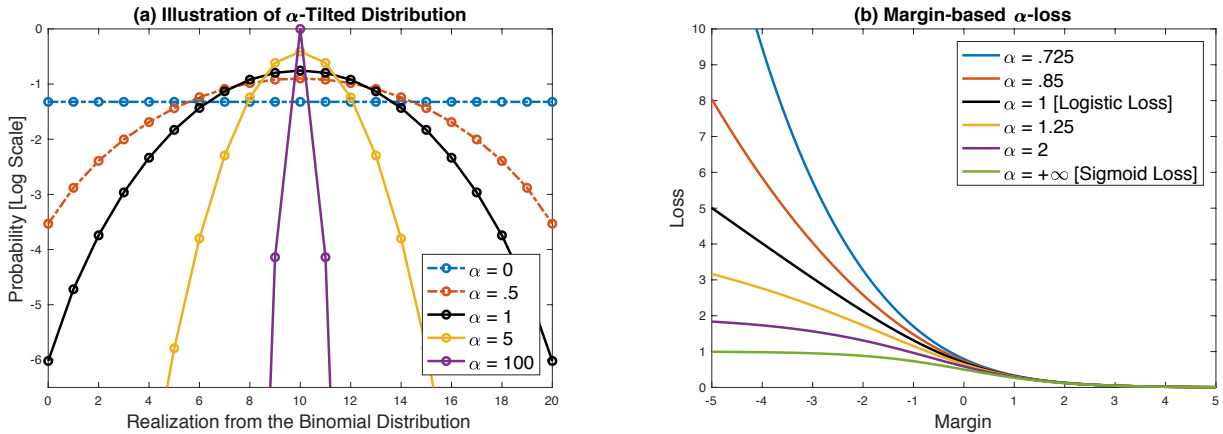


Figure 1: (a) $(20,0.5)$ -Binomial distribution under optimal strategy for different values of α ; (b) margin-based α -loss, as a function of the margin $z = yf(x)$.

The proof of Proposition 1 can be found in [7] and is easily extended to the case where $\alpha \in (0, 1)$.

For binary classification, where $Y \in \{-1, 1\}$, it is common to use classification functions of the form $f : \mathcal{X} \rightarrow \overline{\mathbb{R}}$ such that the classifier, for any given x , outputs the hypothesis (hard decision) $h(x) = \text{sign}(f(x))$ [1–3, 6, 9]. A classification function corresponds to the certainty of an algorithm’s prediction (e.g., SVM). Examples of loss functions that act on classification functions include logistic loss, hinge loss, and square loss.

In addition to classification functions, soft classifiers may also be output by binary classification algorithms. A soft classifier $g : \mathcal{X} \rightarrow [0, 1]$ corresponds to the distribution $P_{\hat{Y}|X}(1|x) := g(x)$. Log-loss, and by extension α -loss, are examples of loss functions which act on soft classifiers. In practice, a soft classifier can be obtained by composing commonly used classification functions with a sigmoid function $\sigma : \overline{\mathbb{R}} \rightarrow [0, 1]$, $\overline{\mathbb{R}} = \mathbb{R} \cup \{\pm\infty\}$, given by

$$\sigma(z) = \frac{1}{1 + e^{-z}}. \quad (4)$$

A large family of loss functions under binary classification are *margin-based* loss functions. [1–3, 9, 15]. A loss function is said to be margin-based if, for all $x \in \mathcal{X}$ and $y \in \mathcal{Y}$, the risk associated to a pair $(y, f(x))$ is given by $\tilde{l}(yf(x))$ for some function $\tilde{l} : \overline{\mathbb{R}} \rightarrow \mathbb{R}_+$. In this case, the risk of the pair $(y, f(x))$ only depends on the product $yf(x)$, where the product $yf(x)$ is called the margin. Observe that a negative margin corresponds to a mismatch between the signs of $f(x)$ and y , i.e., a classification error by f . Similarly, a positive margin corresponds to a match between the signs of $f(x)$ and y , i.e., a correct classification by f .

We now show that α -loss is margin-based over the entire range of $\alpha \in (0, \infty]$; this is also illustrated in Figure 1(b).

Definition 2. The margin-based α -loss, $\tilde{l}^\alpha : \overline{\mathbb{R}} \rightarrow \mathbb{R}_+$, $\alpha \in (0, \infty]$, is

$$\tilde{l}^\alpha(z) := \frac{\alpha}{\alpha - 1} (1 - \sigma(z))^{1-1/\alpha}, \quad \alpha \in (0, 1) \cup (1, \infty), \quad (5)$$

with $\tilde{l}^1(z) = -\log(\sigma(z))$ and $\tilde{l}^\infty(z) = 1 - \sigma(z)$ by continuous extension.

The relationship between a classification function and a soft classifier under α -loss is articulated by the following proposition. It generalizes the result of [6] for the entire range of α .

Proposition 2. Consider a soft classifier $g(x) = P_{\hat{Y}=1|X=x}$. If $f(x) = \sigma^{-1}(g(x))$, then, for every $\alpha \in (0, \infty]$,

$$l^\alpha(y, g(x)) = \tilde{l}^\alpha(yf(x)). \quad (6)$$

Conversely, if f is a classification function, then the set of beliefs $P_{\hat{Y}|X}$ associated to $g(x) := \sigma(f(x))$ satisfies (6). In particular, for every $\alpha \in (0, \infty]$,

$$\min_g \mathbb{E}_{X,Y}(l^\alpha(Y, g(x))) = \min_f \mathbb{E}_{X,Y}(\tilde{l}^\alpha(Yf(X))). \quad (7)$$

The proof of Proposition 2 can be found in [6] and is easily extended to the case where $\alpha \in (0, 1)$.

While the previous result establishes an equivalent margin-based form for α -loss, our next result establishes some of its basic optimization characteristics.

Proposition 3. $\tilde{l}^\alpha : \mathbb{R} \rightarrow \mathbb{R}_+$ is convex for $\alpha \leq 1$ and quasi-convex for $\alpha > 1$.

The proof of Proposition 3 is given in Appendix A.

Finally, we conclude this section with another basic property of α -loss that highlights its suitability for classification. For binary classification and margin-based losses, Bartlett *et al.* in [1] introduce *classification-calibration* as a means to compare the performance of a loss function relative to the 0-1 loss. A margin-based loss function \tilde{l} is classification-calibrated if its minimum conditional risk given $\{X = x\}$ is attained by a z_x^* such that $\text{sign}(z_x^*) = \text{sign}(2\eta(x) - 1)$, where $\eta(x) = P_{Y|X}(1|x)$ is the true posterior. Building upon such a result in [6] for α -loss, the following proposition shows that \tilde{l}^α is classification-calibrated for all α .

Proposition 4. For every $\alpha \in (0, \infty]$, the margin-based α -loss, \tilde{l}^α , is classification-calibrated.

The proof of Proposition 4 is given in Appendix A. In the next section, we consider α -loss in the context of a common machine learning model: logistic regression.

3 Optimization and Generalization

In this section we establish some theoretical properties regarding the performance of α -loss in a logistic regression setting. Towards this end, let $X \in \mathbb{B}_d(1) := \{x \in \mathbb{R}^d : \|x\| \leq 1\}$ be the feature vector, $Y \in \{-1, +1\}$ the label and $S_n = \{(X_i, Y_i) : i = 1, \dots, n\}$ the training dataset where, for each $i \in \{1, \dots, n\}$, the samples (X_i, Y_i) are independently drawn according to an unknown distribution $P_{X,Y}$. We consider the family of soft classifiers $\mathcal{G} = \{g_\theta : \theta \in \mathbb{B}_d(r)\}$ where $r > 0$ and

$$g_\theta(x) = \sigma(\langle \theta, x \rangle), \quad (8)$$

with $\sigma : \mathbb{R} \rightarrow \mathbb{R}$ given as in (4). The α -loss can now be written as

$$l^\alpha(y, g_\theta(x)) = \frac{\alpha}{\alpha - 1} \left[1 - \frac{1+y}{2} g_\theta(x)^{1-1/\alpha} - \frac{1-y}{2} (1 - g_\theta(x))^{1-1/\alpha} \right]. \quad (9)$$

A straightforward computation shows that

$$\frac{\partial}{\partial \theta^j} l^\alpha(y, g_\theta(x)) = \left[\frac{1-y}{2} g_\theta(x) (1 - g_\theta(x))^{1-1/\alpha} - \frac{1+y}{2} g_\theta(x)^{1-1/\alpha} (1 - g_\theta(x)) \right] x^j, \quad (10)$$

where θ^j, x^j denote the j -th components of θ and x , respectively. Thus, the gradient of α -loss is

$$\nabla_\theta l^\alpha(Y, g_\theta(X)) = F_1(\alpha, \theta, X, Y)X, \quad (11)$$

where $F_1(\alpha, \theta, x, y)$ is the expression within brackets in (10). Finally, we define the α -risk R_α as the risk of the α -loss in (9), i.e., $R_\alpha(\theta) := \mathbb{E}_{X,Y}[l^\alpha(Y, g_\theta(X))]$. Observe that, for all $\theta \in \mathbb{B}_d(r)$,

$$R_\infty(\theta) := \mathbb{E}_{X,Y}[l^\infty(Y, g_\theta(X))] = \mathbb{P}[Y \neq \hat{Y}_\theta], \quad (12)$$

where \hat{Y}_θ is a random variable such that $\mathbb{P}[\hat{Y}_\theta = 1 | X = x] = g_\theta(x)$ for all $x \in \mathbb{B}_d(1)$. We define the empirical α -risk \hat{R}_α by

$$\hat{R}_\alpha(\theta) = \frac{1}{n} \sum_{i=1}^n l^\alpha(Y_i, g_\theta(X_i)). \quad (13)$$

3.1 The Optimization Landscape of α -loss

Next we provide some insight regarding the convexity degradation of the optimization landscape as α increases. In order to do so, we rely on a relaxed form of convexity called Strict-Local-Quasi-Convexity. We begin recalling the definition of this notion introduced by Hazan *et al.* in [8]. For $\theta_0 \in \mathbb{R}^d$ and $r > 0$, we let $\mathbb{B}(\theta_0, r) := \{\theta \in \mathbb{R}^d : \|\theta - \theta_0\| \leq r\}$.

Definition 3. Let $\theta, \theta_0 \in \mathbb{R}^d$, $\kappa, \epsilon > 0$. We say that $f : \mathbb{R}^d \rightarrow \mathbb{R}$ is $(\epsilon, \kappa, \theta_0)$ -Strictly-Locally-Quasi-Convex (SLQC) in θ , if at least one of the following applies:

1. $f(\theta) - f(\theta_0) \leq \epsilon$
2. $\|\nabla f(\theta)\| > 0$, and for every $\theta' \in \mathbb{B}(\theta_0, \epsilon/\kappa)$ it holds that $\langle \nabla f(\theta), \theta' - \theta \rangle \leq 0$.

Intuitively, when θ_0 is a minimizer of an $(\epsilon, \kappa, \theta_0)$ -SLQC function f , then, for every θ , either $f(\theta)$ is ϵ -close to optimal or descending along the gradient moves towards θ_0 . This relaxed notion of convexity comes with a natural adaptation of the Gradient Descent (GD) algorithm: Normalized Gradient Descent (NGD) [8] as summarized in Algorithm 1 below.

Algorithm 1 Normalized Gradient Descent (NGD)

- 1: **Input:** Number of Iterations T , $\theta_1 \in \mathbb{R}^d$, learning rate $\eta > 0$
 - 2: **for** $t = 1, 2, \dots, T$ **do**
 - 3: Update: $\theta_{t+1} = \theta_t - \eta \frac{\nabla f_t(\theta_t)}{\|\nabla f_t(\theta_t)\|}$
 - 4: **Return** $\bar{\theta}_T = \arg \min_{\theta_1, \dots, \theta_T} f_t(\theta_t)$
-

Similar to the convergence guarantees for GD on convex problems, NGD comes with natural convergence guarantees for SLQC problems [8, Theorem 4.1] and we summarize it below.

Proposition 5. Fix $\epsilon > 0$, let $f : \mathbb{R}^d \rightarrow \mathbb{R}$, and $\theta^* = \arg \min_{\theta \in \mathbb{R}^d} f(\theta)$. If f is $(\epsilon, \kappa, \theta^*)$ -SLQC in every $\theta \in \mathbb{R}^d$, then running Algorithm 1 with $T \geq \kappa^2 \|\theta_1 - \theta^*\|^2 / \epsilon^2$, and $\eta = \epsilon / \kappa$, we have $f(\bar{\theta}_T) - f(\theta^*) \leq \epsilon$.

For an $(\epsilon, \kappa, \theta_0)$ -SLQC function, a smaller ϵ provides better optimality guarantees. Given $\epsilon > 0$, smaller κ leads to faster optimization as the number of required iterations increases with κ^2 . Finally, by using projections, NGD can be easily adapted to work over convex and closed sets including $\mathbb{B}_d(r)$ (see, for example, [8]).

With the necessary SLQC preliminaries in hand, we now turn our attention to providing guarantees on the SLQC behavior of R_α as a function of α . To this end, in the following lemma, we prove a structural result for general differentiable functions that provides an alternative tractable formulation of the second requirement of SLQC functions in Definition 3. This result provides a useful equivalence between the range of acceptable gradients and the gradient of the point in consideration and is illustrated geometrically in Figure 2. The generality of the result suggests broader applicability. Proof details are in Appendix C.

Lemma 1. Assume that $f : \mathbb{R}^d \rightarrow \mathbb{R}$ is differentiable, $\theta_0 \in \mathbb{R}^d$ and $\gamma > 0$. If $\theta \in \mathbb{R}^d$ is such that $\|\theta - \theta_0\| > \gamma$, then the following are equivalent:

1. $\langle -\nabla f(\theta), \theta' - \theta \rangle \geq 0$ for all $\theta' \in \mathbb{B}_d(\theta_0, \gamma)$,
2. $\langle -\nabla f(\theta), \theta_0 - \theta \rangle \geq \gamma \|\nabla f(\theta)\|$.

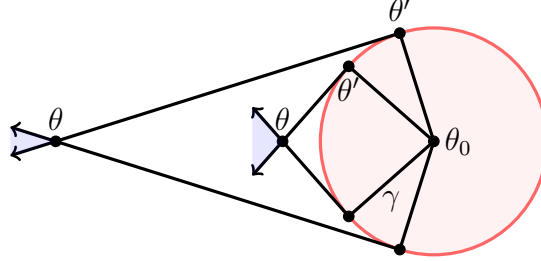


Figure 2: A 2D illustration of the increase in acceptable gradients as θ approaches θ_0 according to the theory of SLQC functions. The region where $\langle -\nabla f(\theta), \theta' - \theta \rangle \geq 0$, for each θ , is depicted by the blue shading. The red region is representative of the $\epsilon/\kappa = \gamma$ ball.

Lemma 1 reformulates the SLQC requirement that the gradient points in the ‘right’ direction into an expression which is reminiscent of a Cauchy-Schwarz inequality. As illustrated in Figure 2, Lemma 1 also captures the fact that the angle of possible gradients at θ increases as θ approaches θ_0 . Intuitively, we find that increasing α is equivalent to moving θ farther away from the ϵ/κ ball (chosen for some initial α_0) as depicted in Figure 2. We now state our second result, which quantifies the degradation of the SLQC constants for α -risk as α increases from 1.

For ease of notation, let

$$K_r := (r + \log 2) \frac{(\sigma(r))^{1-1/(2\sigma(r)-1)}}{(2\sigma(r) - 1)^2} \quad (14)$$

and

$$L_r := \frac{(r + \log 2)^2}{2}. \quad (15)$$

Theorem 1. Let $\epsilon_0, \kappa_0 > 0$ and $\theta_0 \in \mathbb{B}_d(r)$. Suppose that R_{α_0} with $\alpha_0 \in [1, \infty]$ is $(\epsilon_0, \kappa_0, \theta_0)$ -SLQC in θ . Then, R_α with $\alpha \geq \alpha_0$ is $(\epsilon, \kappa, \theta_0)$ -SLQC in θ , where

$$\epsilon = \epsilon_0 + 2L_r(\alpha - \alpha_0) \quad (16)$$

and

$$\kappa = \left(1 + \frac{2L_r(\alpha - \alpha_0)}{\epsilon_0}\right) e^{2K_r(\alpha - \alpha_0)} \kappa_0. \quad (17)$$

The proof of this theorem relies on several lemmas (including Lemma 1) whose proofs are given in Appendix D. The theorem states that increasing the value of α increases the value of ϵ linearly by a factor of $L_r \approx r^2$ and increases the value of κ exponentially through the parameter $K_r \approx r$. Both of these hinder the optimization process and increase the required number of iterations of NGD as stated in Proposition 5. A visual illustration of the degradation of the SLQC constants as α increases is presented in Figure 3 for a two-dimensional Gaussian mixture model (GMM).

Our next result verifies existence of SLQC behavior of R_α for $\alpha \leq 1$ in the logistic model with explicit SLQC constants. To this end, we assume that we are locally-unimodal. That is, locally, R_α has a unique critical point θ^* such that

$$\theta^* = \arg \min_{\theta \in \mathbb{B}_d(r')} R_\alpha(\theta), \quad r' \leq r. \quad (18)$$

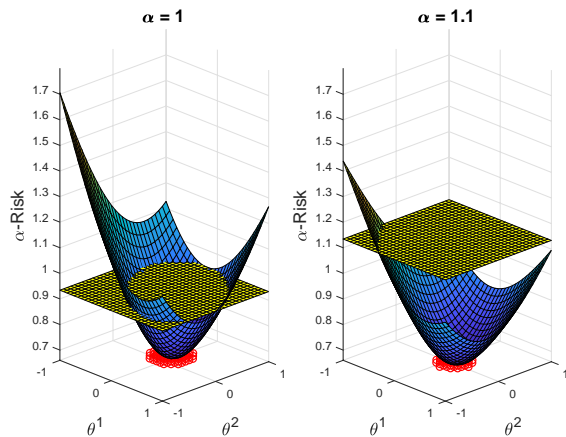


Figure 3: Landscape of α -risk ($\alpha = 1, 1.1$) for a 2D-GMM under logistic regression with $\mathbb{P}[Y = 1] = \mathbb{P}[Y = -1]$, $\mu_{X|Y=-1} = [.5, .5]$, $\mu_{X|Y=1} = [1, 1]$, $\Sigma = [3, .75; .75, 3]$. For $\alpha = 1$, the red region depicts ϵ_0/κ_0 which is calculated using Theorem 2 around θ_0 , where θ_0 is set to be the global minimum of R_1 ; note that $\epsilon_0 = .25$ and is depicted by the yellow plane for $\alpha = 1$. For $\alpha = 1.1$, the red region depicts ϵ/κ about θ_0 and ϵ is depicted by the yellow plane; both quantities are calculated using Theorem 1.

The proof, which can be found in Appendix B, relies on three main facts: (i) R_α is quasi-convex for $\alpha \leq 1$, (ii) R_α is $C_{r',\alpha}$ -Lipschitz where $C_{r',\alpha} := \sigma(r')(1 - \sigma(r'))^{1-1/\alpha}$, and (iii) R_α is assumed to be locally-unimodal.

Theorem 2. *If $0 < \alpha \leq 1$ and $\theta_0 \in \mathbb{B}_d(r')$, then, for every $\epsilon > 0$, the α -risk R_α is $(\epsilon, C_{r',\alpha}, \theta_0)$ -SLQC in $\theta \in \mathbb{B}_d(r')$ where $C_{r',\alpha} = \sigma(r')(1 - \sigma(r'))^{1-1/\alpha}$.*

With this result, Theorem 1 is sufficiently motivated.

Remark 1. *Note that our assumption of local-unimodality for Theorem 2 is akin to the standard assumption that the optimizer is “close-enough” to the desired critical point.*

With Theorems 1 and 2, we observe that the optimization landscape becomes more non-convex as α increases. This could be problematic since the practitioner wants to increase α to obtain more accuracy (to resemble the probability of error). Fortunately as argued in the next section with the saturation phenomenon of α -loss, the optimization slow-down can be mitigated by the fact that one does not need to search too far to obtain the best value of α for a given task.

3.2 Generalization, Accuracy, and Saturation

In this section, we focus on the $\alpha > 1$ setting to highlight three aspects of α -loss: (i) generalization properties, (ii) uniform guarantees on accuracy, (iii) saturation phenomenon. We begin with generalization.

Theorem 3. *If $\alpha \in [1, \infty]$, then, with probability at least $1 - \delta$, for all $\theta \in \mathbb{B}_d(r)$,*

$$|R_\alpha(\theta) - \hat{R}_\alpha(\theta)| \leq C_\alpha \frac{2r}{\sqrt{n}} + 4D_\alpha \sqrt{\frac{2 \log(4/\delta)}{n}}, \quad (19)$$

where, for $\alpha \in (1, \infty)$,

$$C_\alpha = \frac{\alpha}{2\alpha - 1} \left(\frac{\alpha - 1}{2\alpha - 1} \right)^{1-1/\alpha} \quad (20)$$

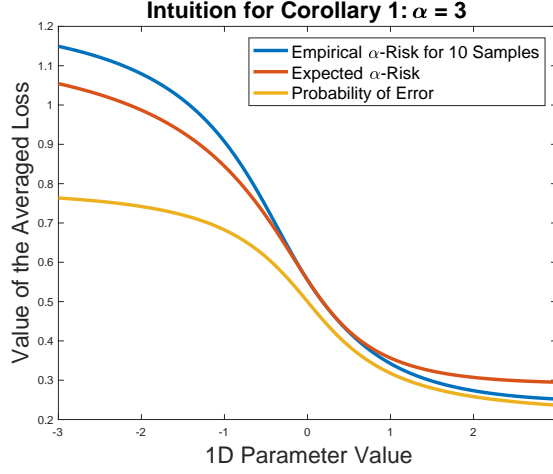


Figure 4: 1D-GMM under logistic regression with $\mathbb{P}[Y = 1] = \mathbb{P}[Y = -1]$, $\mu_1 = 1 = -\mu_{-1}$, and $\sigma_1 = 3$ and $\sigma_{-1} = 1$.

and

$$D_\alpha = \frac{\alpha}{\alpha - 1} \left[1 - (\sigma(-r))^{1-1/\alpha} \right]. \quad (21)$$

It can be verified that C_α and D_α are both monotonically decreasing with α , and are continuously extended such that $C_1 = 1$, $C_\infty = 1/4$, $D_1 = -\log \sigma(-r)$, and $D_\infty = \sigma(r)$. The proof of Theorem 3 relies on classical results in Rademacher complexity; all details are in Appendix E.

Next, we consider uniform guarantees on accuracy. To this end, the following corollary, which stems from Theorem 3, explicitly bounds the accuracy gain using $\alpha > 1$ from the empirical α -risk.

Corollary 1. *If $\alpha \in [1, \infty]$, then, with probability at least $1 - \delta$, for all $\theta \in \mathbb{B}_d(r)$,*

$$|R_\infty(\theta) - \hat{R}_\alpha(\theta)| \leq \frac{r}{2\sqrt{n}} + 4\sqrt{\frac{2 \log(4/\delta)}{n}} + \frac{L_r}{\alpha}, \quad (22)$$

where L_r is given in (15).

Thus, we see that for any $\theta \in \mathbb{B}_d(r)$, increasing α implies that $\hat{R}_\alpha(\theta)$ gets closer to $R_\infty(\theta)$, which is the probability of error of an estimator \hat{Y}_θ with $P(\hat{Y}_\theta = 1 | X = x) = g_\theta(x)$. One can view the third term in (22) as a term which, for a given $\alpha \in [1, \infty]$, penalizes the discrepancy between the (true) α -risk and the probability of error. A visual illustration of this result is provided in Figure 4.

We now turn to the saturation effect of α -loss, which guarantees that, in practice, one does not need to search too far for a good value of α . The following lemma highlights this saturation effect of α -loss for $\alpha \in [1, \infty]$.

Lemma 2. *Let $\theta \in \mathbb{B}_d(r)$ be fixed. If $\alpha, \alpha' \in [1, \infty]$, then*

$$|R_\alpha(\theta) - R_{\alpha'}(\theta)| \leq L_r \left| \frac{1}{\alpha} - \frac{1}{\alpha'} \right|, \quad (23)$$

where L_r is given in (15).

Table 1: Accuracy (Acc.) comparison between log-loss (LL) and α -loss (α -L) at $\alpha^* \in [0.6, 4]$.

Dataset	Optimizer	Architecture	LL Acc.	α -L Acc.	α^*	Rel. Gain%
MNIST	SGD	3-NN	0.981	0.981	1.2	0.038
Fashion MNIST	Adam	3-NN	0.886	0.891	1.5	0.561
CIFAR-10	Adam	CNN-2	0.724	0.729	0.95	0.648

Table 2: Comparison of LL and α -L accuracy (at optimal LR and $\alpha^* \in [0.9, 4]$) with noisy labels.

Dataset	Architecture	Label Flip%	LL Acc.	α -L Acc.	α^*	Rel. Gain %
MNIST	LR	0	0.927	0.934	2.0	0.735
		10	0.913	0.933	2.5	2.190
		20	0.907	0.931	2.0	2.706
CIFAR10	CNN-2	0	0.724	0.729	0.95	0.648
		10	0.693	0.713	1.7	2.906
		20	0.672	0.696	2.0	3.477

Specifically, consider $\alpha' = \infty$, and suppose that $r = 1$ (for a normalized dataset, e.g., MNIST). One finds that with $\alpha = 10$,

$$|R_{10}(\theta) - R_{\infty}(\theta)| \leq \frac{1}{10}. \quad (24)$$

Therefore, $R_{10}(\theta)$ is uniformly upper-bounded from the probability of error by 1/10. Thus, the degradation of the SLQC constants can be mitigated by the fact that one does not have to increase α too much to achieve comparable performance to the probability of error, which is further noted in the next section regarding our experiments for α -loss.

4 Experiments

In this section, we provide experimental illustration of our theoretical results. We perform classification, robustness, and class imbalance experiments to study the efficacy of α -loss in different scenarios. In particular, we use the following datasets: MNIST [22], Fashion MNIST [23], and CIFAR-10 [24]. These datasets come with predefined training and test sets. We divide the original training set into training and validation sets using a 90%-10% breakup, respectively; all training is done in batches of 256. We use a variety of neural network (NN) architectures, as appropriate for the datasets. These include:

- (i) logistic regression (LR) using a two layer NN with Softmax activation;
- (ii) three layer NN (3-NN) with a 128-neuron hidden layer combined with ReLu activation and a Softmax activated output layer;
- (iii) CNN-1: One convolutional (conv) layer with 32 kernels of size 3x3, 1 pooling layer with 2x2 kernels, a 512-size fully connected layer with ReLU activation (dense layer) and an output layer;
- (iv) CNN-2: uses blocks similar to CNN-1 such as pool and dense and has layers in the following order: conv (32 kernels of 3x3), (2x2) Pool, Conv (64 kernels of 3x3), (2x2) Pool, dense, and output.

For a chosen network, we train each of the NN architectures described above for a range of α , each for 100 epochs. For a particular α , the optimal epoch hyperparameter is the one at which the validation loss is minimized; finally, we choose the optimal α^* as the one achieving the best validation accuracy. We use the resulting model parameters (including hyperparameters α^* , optimal epoch value, and learning rate) to report accuracy on the test set. At the outset,

Table 3: Accuracy (Acc.) comparison between log-loss (LL) and α -loss (α -L) for Noisy features at $\alpha^* \in [0.9, 4]$.

Dataset	Architecture	LL Acc.	α -L Acc.	α^*	Rel. Gain
MNIST	LR	0.910	0.917	2.0	0.793
	3-NN	0.972	0.974	1.5	0.249
CIFAR-10	CNN-1	0.510	0.513	0.95	0.636
	CNN-2	0.610	0.627	2.5	2.839

Table 4: Accuracies of less-frequent imbalanced (Imb.) class and both classes (Overall) under log-loss and α -loss for Binary CIFAR-10 with class imbalance. Classes C1 and C2 are the dominant and less-frequent classes with 91% and 9% of all samples, respectively.

Architecture	C1	C2	LL Acc.		α -L Acc.		Rel. Acc. Gain%		α^*
			Imb.	Overall	Imb.	Overall	Imb.	Overall	
CNN-1	Auto	Truck	0.351	0.666	0.416	0.696	18.518	4.501	0.95
	Truck	Auto	0.348	0.664	0.404	0.688	16.091	3.686	0.83
	Cat	Dog	0.111	0.549	0.174	0.573	56.756	4.458	0.9
	Dog	Cat	0.055	0.523	0.074	0.53	34.545	1.337	0.99

we tested both SGD and Adam [25] to compare α -loss and log-loss; for the noisy and class imbalanced datasets we only use Adam. We evaluate the efficacy of α -loss in three scenarios as detailed below. For each, our metric of comparison is the relative gain in accuracy (Acc.) from using α -loss (α -L) over log-loss (LL) computed as $(\alpha\text{-L Acc.} - \text{LL Acc.})/(\text{LL Acc.})$.

4.1 Overall Performance Relative to Log-loss

Table 1 provides a highlight from Table 5 of Appendix F which presents the best α -loss accuracy with respect to log-loss for a given dataset, optimizer, architecture tuple. These results suggest that α -loss, more often than not, offers improvements in accuracy. Indeed, the performance improvements suggest that tuning the extra hyperparameter α is worth the effort for the practitioner.

4.2 Robustness

The robustness of NNs to adversarial influence has recently drawn much attention [26–29]. To this end, we propose the implementation of α -loss to improve the robustness of NNs, and provide two experiments, Noisy Labels and Noisy Features, which indicate that further study of α -loss in this setting is justified.

4.2.1 Noisy Labels

We test the robustness of α -loss to noisy data by flipping a percentage of the labels uniformly at random (from the remaining 9 classes for each label). We vary the flipping percentage from 5-25% in steps of 5%. The results for 0, 10 and 20% are summarized in Table 6 in Appendix F and highlighted in Table 2. The results illustrate that $\alpha > 1$ significantly improves accuracy, which aligns with the information-theoretic interpretations of α -loss as depicted in Proposition 1 and Figure 1.

4.2.2 Noisy Features

We also test the robustness of α -loss to noisy data by altering a percentage of the *pixels* for any given image uniformly at random. We note that the MNIST dataset is comprised of images with 28x28 pixels where each pixel (prior to normalization) takes a value in the range $[0, 255]$; the CIFAR-10 dataset has a similar construction. With regards to our experimental procedure, for the results provided in Table 3, we randomly select 50% of the pixels, add a value uniformly drawn from $[-125, 125]$ to the selected pixels (noise level), and clip the value to 0 or 255 when necessary. More results are provided in Appendix F in Table 9 with different noise levels provided. Overall, we observe performance gains, on average, for $\alpha > 1$.

4.3 Sensitivity to Class Imbalance

We perform class imbalance experiments for a binary-CIFAR and CIFAR-10 datasets. We create binary-CIFAR datasets by considering two class pairs: (i) automobile and truck; and (ii) cat and dog. For each such binary dataset, we reduce the size of one class to 10% such that the affected class is now 9% of whole training and validation set. The test set is unchanged. Both overall accuracy and that for the less-frequent imbalanced class are summarized in Table 4 for CNN-1. Results for CNN-2 are in Appendix F, Table 7; these results suggest that, in general, $\alpha < 1$ achieves significantly better classification (the rare cases for which $\alpha > 1$ hint at a trade-off between accuracy and imbalance). Results for 10% class imbalance for just one CIFAR-10 class with CNN-1 and CNN-2 is summarized in Table 8 of Appendix F; these results reveal significant accuracy gains in detecting the imbalanced class for $\alpha < 1$.

5 Concluding Remarks

We present convexity-robustness trade-offs for a class of surrogate loss functions α -loss, $\alpha \in (0, \infty]$. In practice, we find that the best value of α is dependent on the setting. Since larger α more closely resembles the probability of error, we find that in the noisy setting, the robustness and the quasi-convexity of α -loss for $\alpha > 1$ and its faster generalization capabilities make it more appropriate than log-loss ($\alpha = 1$). For the datasets with class imbalances, we see that α -loss for $\alpha \leq 1$ performs best; this is because the $\alpha < 1$ convex losses place more weight on the outliers (see Figure 1). Our experiments also suggest acceptable gains in accuracy for $\alpha \in [.8, 4]$. For such a range, it is not difficult to do a careful grid search to find the best value of α . The significant performance gains we observe here for noisy and imbalanced datasets could outweigh such (limited range) tuning of an additional (α) hyperparameter. Precise characterization of accuracy gains for $\alpha < 1$, its empirical landscape, and robustness to class imbalance are promising avenues for future work.

Appendices

A Proofs of Margin-Based α -loss Propositions

In this section, we provide proofs of the propositions provided in Section 2.

A.1 Proof of Proposition 3

Proposition 3. $\tilde{l}^\alpha : \mathbb{R} \rightarrow \mathbb{R}_+$ is convex for $\alpha \leq 1$ and quasi-convex for $\alpha > 1$.

Proof. The proof of the case where $\alpha \in [1, \infty]$ can be found in [6]. Now consider $\alpha \in (0, 1)$, in this case

$$\frac{d^2}{dz^2} \tilde{l}^\alpha(z) = \frac{(e^{-z} + 1)^{1/\alpha} e^z (\alpha e^z - \alpha + 1)}{\alpha (e^z + 1)^3}. \quad (25)$$

Observe that the second derivative in (25) is greater than zero for all $z \in \mathbb{R}$, so \tilde{l}^α is a convex function in the margin. \square

A.2 Proof of Proposition 4

The case where $\alpha \in [1, \infty]$ is given in [6].

Before stating the proof of Proposition 4, we provide the full definition of classification-calibration given in [1] for the sake of completeness.

Definition 4 ([1, Definition 1]). A margin-based loss function \tilde{l} is said to be classification-calibrated if, for every $\eta \neq 1/2$,

$$\inf_{f: f(2\eta-1) \leq 0} (\eta \tilde{l}(f) + (1-\eta) \tilde{l}(-f)) > \inf_{f \in \mathbb{R}} (\eta \tilde{l}(f) + (1-\eta) \tilde{l}(-f)). \quad (26)$$

Proposition 4. For every $\alpha \in (0, \infty]$, the margin-based α -loss, \tilde{l}^α , is classification-calibrated.

Proof. For $\alpha \in (0, 1)$, we rely on the following theorem proved by Bartlett *et al.* in [1].

Proposition 6 ([1, Theorem 6]). Let \tilde{l} denote a margin-based loss function and suppose it is a convex function in the margin. Then \tilde{l} is classification-calibrated if and only if it is differentiable at 0 and $\tilde{l}'(0) < 0$.

Observe that \tilde{l}^α for $\alpha \in (0, 1)$ is a convex function of the margin as shown by Proposition 3 and since the loss is monotonically decreasing it satisfies Proposition 6. Thus, \tilde{l}^α is classification-calibrated for $\alpha \in (0, 1)$. The optimal classifier in this region can be found by considering the α -tilted distribution (3) in conjunction with Proposition 2. \square

B Proof of Theorem 2

We first provide the proof of Theorem 2 as it motivates the proof of Theorem 1 and is conceptually much less difficult.

We begin by establishing that the α -risk is Lipschitz.

Lemma 3. If $\alpha \in (0, 1]$, then R_α is $C_{r,\alpha}$ -Lipschitz in $\theta \in \mathbb{B}_d(r)$ where $C_{r,\alpha} = \sigma(r)(1-\sigma(r))^{1-1/\alpha}$, i.e.,

$$|R_\alpha(\theta) - R_\alpha(\theta')| \leq C_{r,\alpha} \|\theta - \theta'\|, \quad \forall \theta, \theta' \in \mathbb{B}_d(r). \quad (27)$$

Proof. We show that R_α is $C_{r,\alpha}$ -Lipschitz in θ by showing that the norm of its gradient ∇R_α is uniformly bounded on $\mathbb{B}_d(r)$ by $C_{r,\alpha}$. Since both $\theta \in \mathbb{B}_d(r)$ and $X \in \mathbb{B}_d(1)$ are bounded, differentiation under the integral sign leads to

$$\begin{aligned}\nabla_\theta R_\alpha(\theta) &= \nabla_\theta \mathbb{E}_{X,Y}[l^\alpha(Y, g_\theta(X))] \\ &= \mathbb{E}_{X,Y}[\nabla_\theta l^\alpha(Y, g_\theta(X))] \\ &= \mathbb{E}_{X,Y}[F_1(\alpha, \theta, X, Y)X].\end{aligned}\tag{28}$$

Since $X \in \mathbb{B}_d(1)$, we obtain that

$$\begin{aligned}\|\nabla_\theta R_\alpha(\theta)\| &= \|\mathbb{E}_{X,Y}[F_1(\alpha, \theta, X, Y)X]\| \\ &\leq \mathbb{E}_{X,Y}[|F_1(\alpha, \theta, X, Y)| \|X\|] \\ &\leq \mathbb{E}_{X,Y}[|F_1(\alpha, \theta, X, Y)|].\end{aligned}\tag{29}$$

By definition, $\mathbb{E}_{X,Y}[|F_1(\alpha, \theta, X, Y)|]$ equals

$$\begin{aligned}\mathbb{E}_{X,Y}\left[\left|\frac{1-Y}{2}g_\theta(X)(1-g_\theta(X))^{1-1/\alpha}\right.\right. \\ \left.\left.-\frac{1+Y}{2}g_\theta(X)^{1-1/\alpha}(1-g_\theta(X))\right|\right].\end{aligned}\tag{30}$$

Using the fact $\alpha \in (0, 1)$, it can be shown that $\sup_{x \in [-r, r]} \sigma(x)(1-\sigma(x))^{1-1/\alpha} = C_{r,\alpha}$. Since

$$g_\theta(z)^{1-1/\alpha}(1-g_\theta(z)) = g_\theta(-z)(1-g_\theta(-z))^{1-1/\alpha}\tag{31}$$

for all $z \in \mathbb{R}$, (30) is easily upper bounded by $C_{r,\alpha}$. \square

We use the following proposition given by Hazan *et al.* in [8] to prove the first theorem.

Proposition 7 ([8]). *If f is G -Lipschitz and a strictly-quasi-convex function, then $\forall \theta, \theta_0 \in \mathbb{R}^d$, $\forall \epsilon > 0$, it holds that f is (ϵ, G, θ_0) -SLQC in θ .*

Now, we present the proof for Theorem 2.

Theorem 2. *If $0 < \alpha \leq 1$ and $\theta_0 \in \mathbb{B}_d(r')$, then, for every $\epsilon > 0$, the α -risk R_α is $(\epsilon, C_{r',\alpha}, \theta_0)$ -SLQC in $\theta \in \mathbb{B}_d(r')$ where $C_{r',\alpha} = \sigma(r')(1-\sigma(r'))^{1-1/\alpha}$.*

Proof. We will prove Theorem 2 by applying Proposition 7. As shown in Lemma 3, R_α is $C_{r,\alpha}$ -Lipschitz for all $\alpha \in (0, 1]$. Next we show quasi-convexity of R_α by level-sets. Since $l^\alpha(y, g_\theta(x))$ is a convex function in θ for $\alpha \leq 1$ and since expectation is a linear operator, we have that R_α is quasi-convex for $0 < \alpha \leq 1$. With regards to strictness, we follow the requirement of Hazan *et al.* [8]. We say that f is strictly-quasi-convex, if it is quasi-convex and its gradients vanish only at the global minima, that is, for all θ' such that $R_\alpha(\theta') > \min_{\theta \in \mathbb{B}_d(r)} R_\alpha(\theta)$, it holds that $\|\nabla R_\alpha(\theta')\| > 0$. Since we assume that we are in the realizable setting where θ^* is the only point for which $\nabla_\theta R_\alpha(\theta^*) = \mathbf{0}$, R_α is strictly-quasi-convex. \square

C Proof of Lemma 1

The following lemma helps to quantify the range of acceptable gradient angles for an SLQC function.

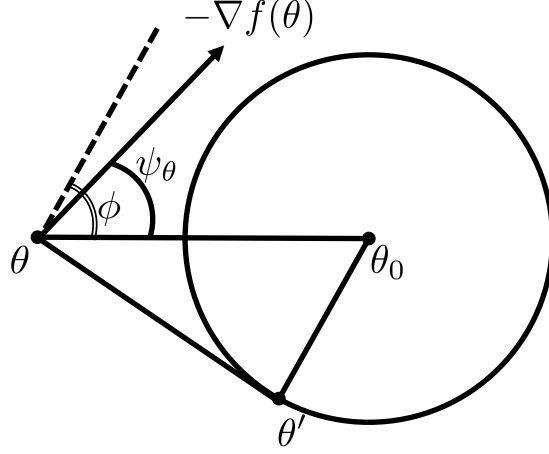


Figure 5: Illustration of the range of acceptable gradients as studied in Lemma 1. Note that the dashed line indicates the worst-case possible negative gradient at θ as required by equation (32).

Lemma 4. Let $\epsilon, \kappa > 0$ and $\theta_0 \in \mathbb{R}^d$. Suppose that f satisfies that, for all θ with $\|\theta - \theta_0\| > \gamma$,

$$\langle -\nabla_{\theta} f(\theta), \theta' - \theta \rangle \geq 0, \quad \forall \theta' \in \mathbb{B}_d(\theta_0, \gamma). \quad (32)$$

Pick $\theta \in \mathbb{R}^d$ such that $\|\theta - \theta_0\| > \gamma$. If ψ_{θ} denotes the angle between $-\nabla f(\theta)$ and $\theta_0 - \theta$, then,

$$\psi_{\theta} \leq \cos^{-1} \left(\frac{\gamma}{\|\theta_0 - \theta\|} \right). \quad (33)$$

Proof. Consider a supporting hyperplane of the ball $\mathbb{B}(\theta_0, \gamma)$ which contains θ , as shown in Figure 5. Let θ' be the intersection between the hyperplane and the ball. Note that for this θ' , $\langle -\nabla_{\theta} f(\theta), \theta' - \theta \rangle \geq 0$ by assumption.

Next, consider the right triangle generated by $\theta_0, \theta', \theta$ and let that ϕ be the acute angle between the perpendicular hyperplane to $\theta' - \theta$ and $\theta_0 - \theta$. By the similarity of the angles, it can be seen that this is the angle at θ_0 of the right triangle. So by Pythagoras' theorem,

$$\phi = \cos^{-1} \left(\frac{\gamma}{\|\theta_0 - \theta\|} \right). \quad (34)$$

By assumption (32), it can be shown that $\psi_{\theta} \leq \phi$. Furthermore, θ' as chosen here minimizes ϕ , i.e., any other $\theta' \in \mathbb{B}(\theta_0, \gamma)$ would impose a less restrictive constraint on the magnitude of ψ_{θ} by making ϕ larger. \square

We now provide the proof of Lemma 1.

Lemma 1. Assume that $f : \mathbb{R}^d \rightarrow \mathbb{R}$ is differentiable, $\theta_0 \in \mathbb{R}^d$ and $\gamma > 0$. If $\theta \in \mathbb{R}^d$ is such that $\|\theta - \theta_0\| > \gamma$, then the following are equivalent:

1. $\langle -\nabla f(\theta), \theta' - \theta \rangle \geq 0$ for all $\theta' \in \mathbb{B}_d(\theta_0, \gamma)$,
2. $\langle -\nabla f(\theta), \theta_0 - \theta \rangle \geq \gamma \|\nabla f(\theta)\|$.

Proof. Let $\psi = \psi_{\theta}$ and ϕ as in the proof of the previous lemma. It follows that $0 \leq \psi \leq \frac{\pi}{2}$ and $\phi = \cos^{-1} \left(\frac{\gamma}{\|\theta - \theta_0\|} \right)$. By the definition of inner product, it follows that

$$\cos(\psi) \|\theta - \theta_0\| \|\nabla f(\theta)\| = \langle -\nabla f(\theta), \theta_0 - \theta \rangle. \quad (35)$$

Rearranging we get

$$\psi = \cos^{-1} \left(\frac{\langle -\nabla f(\theta), \theta_0 - \theta \rangle}{\|\theta - \theta_0\| \|\nabla f(\theta)\|} \right) \in [0, \pi]. \quad (36)$$

Further, $\psi \leq \phi$ by the previous lemma. This requirement is equivalent to

$$\cos^{-1} \left(\frac{\langle -\nabla f(\theta), \theta_0 - \theta \rangle}{\|\theta - \theta_0\| \|\nabla f(\theta)\|} \right) \leq \cos^{-1} \left(\frac{\gamma}{\|\theta - \theta_0\|} \right). \quad (37)$$

Since \cos^{-1} is a monotonically decreasing function, the previous condition is equivalent to

$$\langle -\nabla f(\theta), \theta_0 - \theta \rangle \geq \gamma \|\nabla f(\theta)\| \geq 0. \quad (38)$$

Notice that the steps are reversible so we have both directions. \square

D Proof of Theorem 1

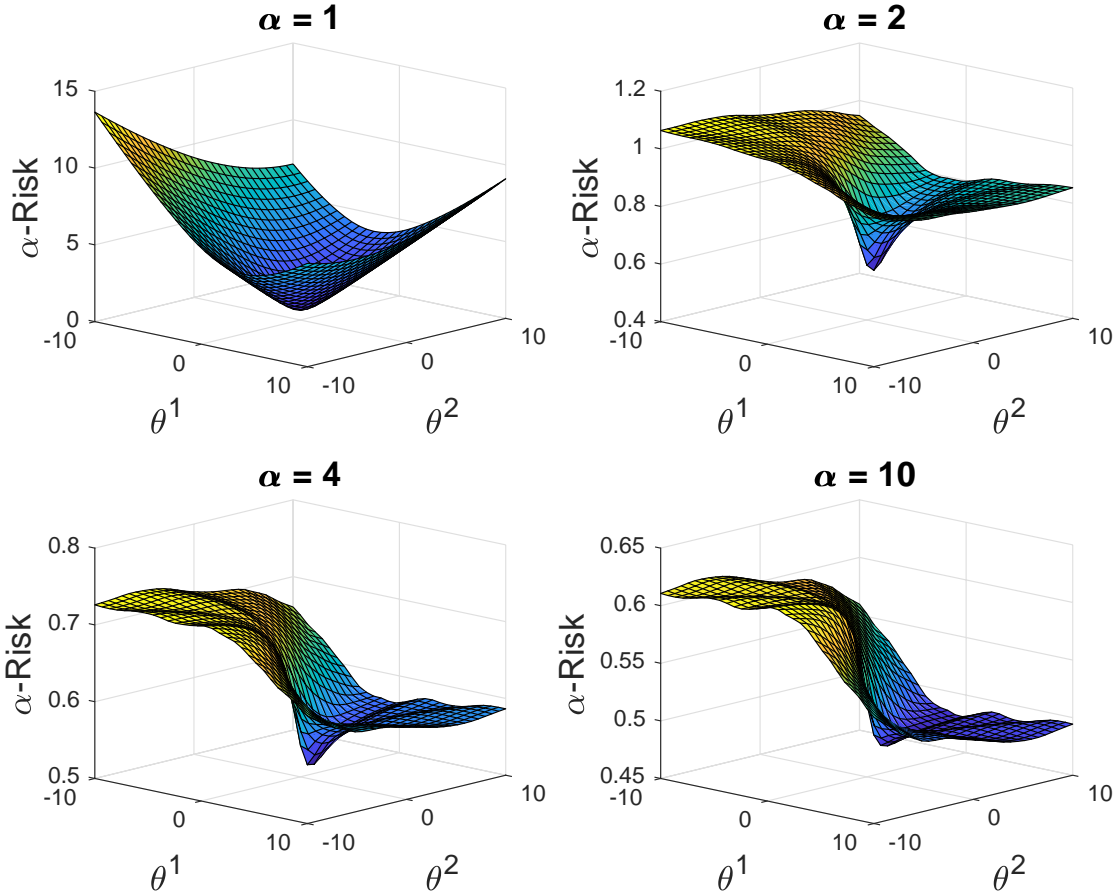


Figure 6: Landscape of α -loss (R_α for $\alpha = 1, 2, 4, 10$) for a 2D-GMM under logistic regression with $\mathbb{P}[Y = 1] = \mathbb{P}[Y = -1]$, $\mu_{X|Y=-1} = [.5, .5]$, $\mu_{X|Y=1} = [1, 1]$, $\Sigma = [1, .5; .5, 3]$.

In Figure 6, we provide an illustration of the evolution of the landscape as α increases. Theorem 1 attempts to capture this evolution with the theory of SLQC functions. We begin by proving a set of lemmas which are necessary for the proof of Theorem 1.

D.1 Auxiliary Lemmas

The first lemma shows that the α -risk is L_r -Lipschitz as a function of α .

Lemma 5. *If $\alpha \in [1, \infty]$, then $|R_\alpha(\theta) - R_{\alpha'}(\theta)| \leq L_r |\alpha - \alpha'|$, where $L_r = \frac{(r + \log 2)^2}{2}$.*

Proof. To show that R_α is L_r -Lipschitz in α , it suffices to show that $\frac{d}{d\alpha} R_\alpha(\theta) \leq L_r$. Observe that

$$\frac{d}{d\alpha} R_\alpha(\theta) = \frac{d}{d\alpha} \mathbb{E}[l^\alpha(Y, g_\theta(X))] = \mathbb{E} \left[\frac{d}{d\alpha} l^\alpha(Y, g_\theta(X)) \right], \quad (39)$$

where the second equality follows since we assume well-behaved integrals. We may rewrite this expression as

$$\begin{aligned} \mathbb{E} \left[\frac{d}{d\alpha} l^\alpha(Y, g_\theta(X)) \right] &= P_1 \mathbb{E}_{X|Y=1} \left[\frac{d}{d\alpha} l^\alpha(1, g_\theta(X)) \right] \\ &\quad + P_{-1} \mathbb{E}_{X|Y=-1} \left[\frac{d}{d\alpha} l^\alpha(-1, g_\theta(X)) \right]. \end{aligned} \quad (40)$$

Consider without loss of generality the expression in the first brackets for a fixed x . We denote this expression as

$$f(\alpha, \theta, x) = \frac{d}{d\alpha} \frac{\alpha}{\alpha - 1} [1 - g_\theta(x)^{1-1/\alpha}]. \quad (41)$$

It can be shown that

$$\begin{aligned} f(\alpha, \theta, x) &= \frac{1 - g_\theta(x)^{1-1/\alpha}}{\alpha - 1} - \frac{(\log g_\theta(x)) g_\theta(x)^{1-1/\alpha}}{\alpha(\alpha - 1)} \\ &\quad - \frac{\alpha(1 - g_\theta(x)^{1-1/\alpha})}{(\alpha - 1)^2}. \end{aligned} \quad (42)$$

By L'Hopital's rule, we have that

$$f(1, \theta, x) = -\frac{(\log g_\theta(x))^2}{2}. \quad (43)$$

Further, it can be shown that $f(\alpha, \theta, x)$ is monotonically decreasing in α . Thus,

$$|f(\alpha, \theta, x)| \leq |f(1, \theta, x)| \leq \left| \frac{(\log g_\theta(x))^2}{2} \right| \leq \frac{(r + \log 2)^2}{2}. \quad (44)$$

Upon plugging (44) into (40), the expectation sums to 1 and we achieve the desired bound on $\frac{d}{d\alpha} R_\alpha(\theta)$. \square

The second lemma shows that the gradient of the α -risk with respect to the parameter vector is K_r -Lipschitz as a function of α .

Lemma 6. *If $\alpha \in [1, \infty]$, then*

$$\|\nabla R_\alpha(\theta) - \nabla R_{\alpha'}(\theta)\| \leq K_r |\alpha - \alpha'|, \quad (45)$$

where

$$K_r = (r + \log 2) \frac{(\sigma(r))^{1-1/(2\sigma(r)-1)}}{(2\sigma(r) - 1)^2}. \quad (46)$$

Proof. By the linearity of the expectation we can bound $\|\nabla R_\alpha(\theta) - \nabla R_{\alpha'}(\theta)\|$ as

$$\begin{aligned} & \|\nabla R_\alpha(\theta) - \nabla R_{\alpha'}(\theta)\| \\ &= \|\mathbb{E}[(F_1(\alpha, \theta, X, Y) - F_1(\alpha', \theta, X, Y))X]\| \\ &\leq \mathbb{E}[|(F_1(\alpha, \theta, X, Y) - F_1(\alpha', \theta, X, Y))||X|] \\ &= \mathbb{E}[|(F_1(\alpha, \theta, X, Y) - F_1(\alpha', \theta, X, Y))|], \end{aligned} \quad (47)$$

since X has bounded support. Here, we explore the Lipschitzianity of F_1 . To do so, we calculate the maximum value of $\frac{d}{d\alpha}F_1(\alpha, \theta, x, y)$. Consider

$$\begin{aligned} F_1(\alpha, \theta, x, y) &= \frac{1-y}{2}g_\theta(x)(1-g_\theta)^{1-1/\alpha} \\ &\quad - \frac{1+y}{2}g_\theta^{1-1/\alpha}(1-g_\theta(x)). \end{aligned} \quad (48)$$

For any pair (x, y) , only one term is active, so let $(x, y) = (x, -1)$ without loss of generality. Thus,

$$F_1(\alpha, \theta, x, -1) = -g_\theta^{1-1/\alpha}(1-g_\theta(x)). \quad (49)$$

In particular, we have that

$$\begin{aligned} \frac{d}{d\alpha}F_1(\alpha, \theta, x, -1) &= -g_\theta^{1-1/\alpha} \frac{1}{\alpha^2} \log(g_\theta(x))(1-g_\theta(x)) \\ &= g_\theta^{1-1/\alpha} \frac{1}{\alpha^2} \log(1+e^{-\theta x})g_\theta(-x). \end{aligned} \quad (50)$$

To maximize the derivative, we maximize some of its factors individually. Notice that $g_\theta(-x) \leq 1$ and $\log(1+e^{-\theta x}) \leq \log(1+e^r) \leq r + \log 2$. Next, consider $f(\alpha, \theta, x) = \frac{g_\theta(x)^{1-1/\alpha}}{\alpha^2}$. Observe that since $f(\alpha, \theta, x)$ is monotonic in $g_\theta(x)$, it follows that

$$\max_{\theta \cdot x} f(\alpha, \theta, x) = \frac{\left(\frac{e^r}{e^r+1}\right)^{1-1/\alpha}}{\alpha^2}. \quad (51)$$

Now, we maximize this expression in terms of α . To do this, we observe that the expression is monotonic, so we take a derivative and set it equal to zero. After some basic computations we have that

$$\frac{d}{d\alpha} \frac{\left(\frac{e^r}{e^r+1}\right)^{1-1/\alpha}}{\alpha^2} = 0 \quad (52)$$

implies that $\alpha^* = 2\frac{e^r}{e^r+1} - 1$. Therefore, the Lipschitz constant for F_1 is

$$K_r = (r + \log 2) \frac{\left(\frac{e^r}{e^r+1}\right)^{1-1/\alpha^*}}{(\alpha^*)^2}, \quad (53)$$

where $\alpha^* = 2\frac{e^r}{e^r+1} - 1$. Thus,

$$\|\nabla R_\alpha(\theta) - \nabla R_{\alpha'}(\theta)\| \leq K_r |\alpha - \alpha'|. \quad (54)$$

□

We prove Lemma 7.

Lemma 7. *Let $\epsilon, \kappa > 0$ and $\theta_0 \in \mathbb{B}_d(r)$. If R_α is $(\epsilon, \kappa, \theta_0)$ -SLQC in θ and $|\alpha - \alpha'| \leq 1/(2K_r)$, then $R_{\alpha'}$ is $(\epsilon', \kappa', \theta_0)$ -SLQC in θ with $\epsilon' = \epsilon + 2|\alpha - \alpha'|L_r$ and $\epsilon'/\kappa' = (1 - 2K_r|\alpha - \alpha'|)\epsilon/\kappa$.*

Proof. We consider two cases.

Case 1: If θ is such that $R_\alpha(\theta) - R_\alpha(\theta_0) \leq \epsilon$, then,

$$\begin{aligned} R_{\alpha'}(\theta) - R_{\alpha'}(\theta_0) &= R_{\alpha'}(\theta) - R_\alpha(\theta) + R_\alpha(\theta) - R_\alpha(\theta_0) + R_\alpha(\theta_0) - R_{\alpha'}(\theta_0) \\ &\leq L_r|\alpha - \alpha'| + \epsilon + L_r|\alpha - \alpha'|. \end{aligned} \quad (55)$$

This implies that $\epsilon' \geq \epsilon + 2L_r|\alpha - \alpha'|$. Thus, $R_{\alpha'}(\theta) - R_{\alpha'}(\theta_0) \leq \epsilon'$.

Case 2: Suppose θ is such that $R_\alpha(\theta) - R_\alpha(\theta_0) > \epsilon$. Let $\gamma = \frac{\epsilon}{\kappa}$. By Lemma 1, we want to prove that

$$\langle -\nabla R_{\alpha'}(\theta), \theta_0 - \theta \rangle \geq \gamma' \|\nabla R_{\alpha'}(\theta)\|, \quad (56)$$

for some $\gamma' > 0$. Recall by the Cauchy-Schwarz inequality that for any three vectors it holds that

$$\begin{aligned} \langle -\nabla R_{\alpha'}(\theta), \theta_0 - \theta \rangle &\geq \langle -\nabla R_\alpha(\theta), \theta_0 - \theta \rangle \\ &\quad - \|\nabla R_\alpha(\theta) - \nabla R_{\alpha'}(\theta)\| \|\theta_0 - \theta\|. \end{aligned} \quad (57)$$

By Lemma 6 it follows that

$$\langle -\nabla R_{\alpha'}(\theta), \theta_0 - \theta \rangle \geq \langle -\nabla R_\alpha(\theta), \theta_0 - \theta \rangle - K_r|\alpha - \alpha'|\gamma. \quad (58)$$

Since R_α is SLQC, by Lemma 1 we have

$$\langle -\nabla R_{\alpha'}(\theta), \theta_0 - \theta \rangle \geq \gamma \|\nabla R_\alpha(\theta)\| - K_r|\alpha - \alpha'|\gamma. \quad (59)$$

By the reverse triangle inequality and since $\nabla R_\alpha(\theta)$ is K_r -Lipschitz in α we have that

$$\langle -\nabla R_{\alpha'}(\theta), \theta_0 - \theta \rangle \geq \gamma \|\nabla R_{\alpha'}(\theta)\| - 2K_r|\alpha - \alpha'|\gamma. \quad (60)$$

We want $\gamma \|\nabla R_{\alpha'}(\theta)\| - 2K_r|\alpha - \alpha'|\gamma \geq \gamma' \|\nabla R_{\alpha'}(\theta)\|$ for some γ' . To achieve this, we rearrange the previous equation and obtain

$$\gamma' \leq \gamma - \frac{2\gamma K_r}{\|\nabla R_{\alpha'}(\theta)\|}. \quad (61)$$

Recall that $\|\nabla R_{\alpha'}(\theta)\| \leq |F_1(\alpha', \theta, X, Y)| \|X\| \leq 1$ for $\alpha > 1$. So, we have

$$\gamma' \leq \gamma(1 - 2K_r|\alpha - \alpha'|), \quad (62)$$

which is valid only when $|\alpha - \alpha'| \leq \frac{1}{2K_r}$. \square

D.2 Proof of Theorem 1

With the necessary lemmas behind us, we now provide the proof of Theorem 1.

Theorem 1. *Let $\epsilon_0, \kappa_0 > 0$ and $\theta_0 \in \mathbb{B}_d(r)$. Suppose that R_{α_0} with $\alpha_0 \in [1, \infty]$ is $(\epsilon_0, \kappa_0, \theta_0)$ -SLQC in θ . Then, R_α with $\alpha \geq \alpha_0$ is $(\epsilon, \kappa, \theta_0)$ -SLQC in θ , where*

$$\epsilon = \epsilon_0 + 2L_r(\alpha - \alpha_0) \quad (63)$$

and

$$\kappa = \left(1 + \frac{2L_r(\alpha - \alpha_0)}{\epsilon_0}\right) e^{2K_r(\alpha - \alpha_0)} \kappa_0. \quad (64)$$

Proof. For ease of notation, let $\alpha - \alpha_0 = \Delta$. Assume that $n \in \mathbb{N}$ satisfies $n > 2K_r\Delta$. For $i \in [n]$, let $\alpha_i = \alpha_0 + \frac{i}{n}\Delta$. We denote $\epsilon_i^{(j)}$ as the i -th ϵ in a j -step sequence; this is the same for κ as well.

Assume that R_{α_i} is $(\epsilon_i^{(n)}, \kappa_i^{(n)}, \theta_0)$ -SLQC in θ . Indeed, for $i = 1$, R_{α_1} is $(\epsilon_1^{(n)}, \kappa_1^{(n)}, \theta_0)$ -SLQC in θ by Lemma 7, where

$$\epsilon_1^{(n)} = \epsilon_0 + \frac{2\Delta L_r}{n} \quad (65)$$

and

$$\frac{\epsilon_1^{(n)}}{\kappa_1^{(n)}} = \frac{\epsilon_0}{\kappa_0} \left(1 - \frac{2\Delta K_r}{n} \right). \quad (66)$$

Since for any $i \in [n-1]$, $\alpha_{i+1} = \alpha_i + \frac{\Delta}{n}$, we can further apply Lemma 7 to obtain

$$\epsilon_{i+1}^{(n)} = \epsilon_i^{(n)} + \frac{2\Delta L_r}{n} \quad (67)$$

and

$$\frac{\epsilon_{i+1}^{(n)}}{\kappa_{i+1}^{(n)}} = \left(1 - \frac{2K_r\Delta}{n} \right) \frac{\epsilon_i^{(n)}}{\kappa_i^{(n)}}. \quad (68)$$

Therefore, by applying equations (67) and (68) iteratively, for $i = n$, we obtain

$$\epsilon_n^{(n)} = \epsilon_0 + 2\Delta L_r \quad (69)$$

and

$$\frac{\epsilon_n^{(n)}}{\kappa_n^{(n)}} = \left(1 - \frac{2\Delta K_r}{n} \right)^n \frac{\epsilon_0}{\kappa_0}. \quad (70)$$

Since $\epsilon_n^{(n)}$ does not depend on n , we may rewrite it as

$$\epsilon_n^{(n)} = \epsilon = \epsilon_0 + 2\Delta L_r. \quad (71)$$

Considering $\frac{\epsilon_n^{(n)}}{\kappa_n^{(n)}}$ and taking the limit as $n \rightarrow \infty$, we find that

$$\frac{\epsilon}{\kappa} = \lim_{n \rightarrow \infty} \frac{\epsilon_n^{(n)}}{\kappa_n^{(n)}} \quad (72)$$

$$= \lim_{n \rightarrow \infty} \left(1 - \frac{2\Delta K_r}{n} \right)^n \frac{\epsilon_0}{\kappa_0} \quad (73)$$

$$= e^{-2\Delta K_r} \frac{\epsilon_0}{\kappa_0}. \quad (74)$$

Notice that for any $x \in \mathbb{R}$ and $n \in \mathbb{N}$,

$$\left(1 + \frac{x}{n} \right)^n \leq e^x. \quad (75)$$

Thus, for any $n \in \mathbb{N}$,

$$\left(1 - \frac{2\Delta K_r}{n} \right)^n \frac{\epsilon_0}{\kappa_0} \leq e^{-2\Delta K_r} \frac{\epsilon_0}{\kappa_0}, \quad (76)$$

so we pick $e^{-2\Delta K_r} \frac{\epsilon_0}{\kappa_0}$ as the optimal radius since it's the largest and, therefore, has the least optimization time according to NGD. Substituting equation (71) into (74) and solving equation (74) for κ , we find that

$$\kappa = \left(1 + \frac{2\Delta L_r}{\epsilon_0} \right) e^{2\Delta K_r} \kappa_0. \quad (77)$$

□

E Proof of Theorem 3

In this section, we provide supplementary material regarding the tools from Rademacher complexity we employ and a lemma which is necessary in the proof of our generalization result.

Recall that the Rademacher distribution is the uniform distribution on the set $\{-1, +1\}$.

Definition 5 ([30, Chapter 26]). *Given a nonempty set $A \subset \mathbb{R}^m$, its Rademacher complexity is defined by*

$$\mathcal{R}(A) := \mathbb{E} \left(\sup_{a \in A} \frac{1}{m} \langle \sigma, a \rangle \right), \quad (78)$$

where $\sigma = (\sigma_1, \sigma_2, \dots, \sigma_m)$ with $\sigma_1, \sigma_2, \dots, \sigma_m$ i.i.d. Rademacher random variables.

The next two lemmas and proposition are classical results in generalization theory, see, e.g., [30].

Lemma 8 (Contraction Lemma). *Let $f_1, \dots, f_m : \mathbb{R} \rightarrow \mathbb{R}$ be Lipschitz functions with common constant $\rho \geq 0$. If $f = (f_1, \dots, f_m)$ and $A \subset \mathbb{R}^m$, then $\mathcal{R}(f(A)) \leq \rho \mathcal{R}(A)$.*

Lemma 9. *Let $S_n = (\mathbf{x}_1, \dots, \mathbf{x}_n)$ be vectors in \mathbb{R}^d . Define $\mathcal{H}' \circ S_n = \{(\langle \mathbf{w}, \mathbf{x}_1 \rangle, \dots, \langle \mathbf{w}, \mathbf{x}_n \rangle) : \|\mathbf{w}\| \leq r\}$. Then,*

$$\mathcal{R}(\mathcal{H}' \circ S_n) \leq \frac{r \max_i \|\mathbf{x}_i\|_\infty}{\sqrt{n}}. \quad (79)$$

Proposition 8. *Assume that for all z and $h \in \mathcal{H}$ we have that $|l(h, z)| \leq D$, where $l : \mathcal{H} \times \mathcal{Z} \rightarrow \mathbb{R}_+$ is the loss function. Then, with probability at least $1 - \delta$, for all $h \in \mathcal{H}$,*

$$R_l(h) - \hat{R}_l(h) \leq 2\mathcal{R}(l \circ \mathcal{H} \circ S_n) + 4D \sqrt{\frac{2 \ln(4/\delta)}{n}}, \quad (80)$$

where $R_l(h)$ and $\hat{R}_l(h)$ denote the true risk and empirical risk of l , respectively.

Note that one can obtain a two-sided version of the inequality in (80) since the proof of Proposition 8 relies on the symmetrization trick (see Lemma 26.2 of [30]). We use the two-sided version for Theorem 3 and Corollary 1.

We now present the following lemma which we will use for our generalization bound.

Lemma 10. $|\tilde{l}^\alpha(z) - \tilde{l}^\alpha(z')| \leq C_\alpha |z - z'|$, where $C_\alpha = \frac{\alpha}{2\alpha - 1} \left(\frac{\alpha - 1}{2\alpha - 1} \right)^{1-1/\alpha}$ for $\alpha \in [1, \infty]$.

Proof. For $\alpha = 1$, $\frac{d}{dz} l^1(z) = \frac{e^{-z}}{1 + e^{-z}} \leq 1$. For $\alpha = \infty$, $\frac{d}{dz} l^\infty(z) = \frac{e^z}{(e^z + 1)^2} \leq \frac{1}{4}$. For $\alpha \in (1, \infty)$, we have

$$\begin{aligned} \frac{d}{dz} l^\alpha(z) &= \frac{d}{dz} \frac{\alpha}{\alpha - 1} (1 - \sigma(z))^{1-1/\alpha} \\ &= \sigma(z)^{2-1/\alpha} - \sigma(z)^{1-1/\alpha}. \end{aligned} \quad (81)$$

Maximizing this expression over z (taking the derivative and setting it equal to zero), we find that $z^* = \sigma^{-1} \left(\frac{1 - 1/\alpha}{2 - 1/\alpha} \right)$. Note that in our setting $z = y \langle \theta, x \rangle$, which is bounded. However, any bound we obtain in the unrestricted case will apply in our restricted setting. Thus,

$$\begin{aligned} \frac{d}{dz} l^\alpha(z^*) &= \left(\frac{1 - 1/\alpha}{2 - 1/\alpha} \right)^{2-1/\alpha} - \left(\frac{1 - 1/\alpha}{2 - 1/\alpha} \right)^{1-1/\alpha} \\ &= -\frac{\alpha}{2\alpha - 1} \left(\frac{\alpha - 1}{2\alpha - 1} \right)^{1-1/\alpha}. \end{aligned} \quad (82)$$

So, we take the absolute value to obtain

$$C_\alpha = \frac{\alpha}{2\alpha - 1} \left(\frac{\alpha - 1}{2\alpha - 1} \right)^{1-1/\alpha}. \quad (83)$$

By L'Hospital's rule it can be shown that $C_1 = 1$ and by plugging in $\alpha = \infty$ we can see that $C_\infty = \frac{1}{4}$. Thus, $\frac{1}{4} \leq C_\alpha \leq 1$. Note that it is easily shown that C_α is monotonically decreasing in α . \square

E.1 Proof of Theorem 3

We provide explicit forms of the constants C_α and D_α for reference:

$$C_\alpha = \begin{cases} \frac{\alpha}{2\alpha - 1} \left(\frac{\alpha - 1}{2\alpha - 1} \right)^{1-1/\alpha} & \text{for } \alpha \in (1, \infty) \\ 1 & \text{for } \alpha = 1 \\ 1/4 & \text{for } \alpha = \infty. \end{cases} \quad (84)$$

and

$$D_\alpha = \begin{cases} \frac{\alpha}{\alpha - 1} \left[1 - \left(\frac{1}{1 + e^r} \right)^{1-1/\alpha} \right] & \text{for } \alpha \in (1, \infty) \\ \log(1 + e^r) & \text{for } \alpha = 1 \\ \frac{e^r}{e^r + 1} & \text{for } \alpha = \infty. \end{cases} \quad (85)$$

We prove Theorem 3 using the tools presented above.

Theorem 3. *If $\alpha \in [1, \infty]$, then, with probability at least $1 - \delta$, for all $\theta \in \mathbb{B}_d(r)$,*

$$|R_\alpha(\theta) - \hat{R}_\alpha(\theta)| \leq C_\alpha \frac{2r}{\sqrt{n}} + 4D_\alpha \sqrt{\frac{2 \log(4/\delta)}{n}}, \quad (86)$$

where $C_\alpha = \frac{\alpha}{2\alpha - 1} \left(\frac{\alpha - 1}{2\alpha - 1} \right)^{1-1/\alpha}$ and $D_\alpha = \frac{\alpha}{\alpha - 1} \left[1 - (\sigma(-r))^{1-1/\alpha} \right]$, for $\alpha \in (1, \infty)$.

Proof. By Proposition 2 in Sypherd, et al. (2019), which gives a relation between α -loss and its margin-based form, we have

$$\begin{aligned} \mathcal{R}(l^\alpha \circ \mathcal{G} \circ S_n) &= \mathbb{E} \left(\sup_{g_\theta \in \mathcal{H}} \frac{1}{n} \sum_{i=1}^n \sigma_i l^\alpha(y_i, g_\theta(x_i)) \right) \\ &= \mathbb{E} \left(\sup_{\theta \in \mathbb{B}_d(r)} \frac{1}{n} \sum_{i=1}^n \sigma_i \tilde{l}^\alpha(y_i \langle \theta, x_i \rangle) \right). \end{aligned} \quad (87)$$

The right-hand-side of (87) can be rewritten as

$$\begin{aligned} &\mathbb{E} \left(\sup_{\theta \in \mathbb{B}_d(r)} \frac{1}{n} \sum_{i=1}^n \sigma_i \tilde{l}^\alpha(y_i \langle \theta, x_i \rangle) \right) \\ &= \mathcal{R}(\{\tilde{l}^\alpha(y_1 \langle \theta, x_1 \rangle), \dots, \tilde{l}^\alpha(y_n \langle \theta, x_n \rangle) : \theta \in \mathbb{B}_d(r)\}). \end{aligned} \quad (88)$$

By Lemma 10, we know that $\tilde{l}^\alpha(z)$ is a Lipschitz function in z . Thus, we may apply Lemma 8 (Contraction Lemma) to obtain

$$\begin{aligned} & \mathcal{R}(\{\tilde{l}^\alpha(y_1\langle\theta, x_1\rangle), \dots, \tilde{l}^\alpha(y_n\langle\theta, x_n\rangle) : \theta \in \mathbb{B}_d(r)\}) \\ & \leq C_\alpha \mathcal{R}(\{(y_1\langle\theta, x_1\rangle), \dots, y_n\langle\theta, x_n\rangle) : \theta \in \mathbb{B}_d(r)\}). \end{aligned} \quad (89)$$

We absorb y_i into its corresponding x_i and apply Lemma 9 to obtain

$$C_\alpha \mathcal{R}(\{(y_1\langle\theta, x_1\rangle), \dots, y_n\langle\theta, x_n\rangle) : \theta \in \mathbb{B}_d(r)\}) \leq C_\alpha \frac{r}{\sqrt{n}}, \quad (90)$$

which follows since we assume that X is supported by the unit ball. In order to apply Proposition 8, it is easily shown that for $\alpha \in [1, \infty]$

$$\max_{z \in [-r, r]} \tilde{l}^\alpha(z) \leq D_\alpha. \quad (91)$$

Thus, we apply Proposition 8 to achieve the desired result. \square

E.2 Proof of Corollary 1

The following lemma establishes that α -risk is Lipschitz continuous at infinity. Its proof is left to the reader as it is similar to the proof of Lemma 5.

Lemma 11. *Let $\theta \in \mathbb{B}_d(r)$ be fixed. If $\alpha, \alpha' \in [1, \infty]$, then*

$$|R_\alpha(\theta) - R_{\alpha'}(\theta)| \leq L_r \left| \frac{1}{\alpha} - \frac{1}{\alpha'} \right|, \quad (92)$$

where $L_r = \frac{(r + \log 2)^2}{2}$.

We now provide the proof of Corollary 1.

Corollary 1. *If $\alpha \in [1, \infty]$, then, with probability at least $1 - \delta$, for all $\theta \in \mathbb{B}_d(r)$,*

$$|R_\infty(\theta) - \hat{R}_\alpha(\theta)| \leq \frac{r}{2\sqrt{n}} + 4\sqrt{\frac{2 \log(4/\delta)}{n}} + \frac{L_r}{\alpha}, \quad (93)$$

where L_r is given in (15).

Proof. Consider the expression, $R_\infty(\theta) - \hat{R}_\alpha(\theta)$. Since $\hat{R}_\infty(\theta) \leq \hat{R}_\alpha(\theta)$ for all $\theta \in \mathbb{B}_d(r)$, the following holds

$$R_\infty(\theta) - \hat{R}_\alpha(\theta) \leq R_\infty(\theta) - \hat{R}_\infty(\theta) \leq \frac{r}{2\sqrt{n}} + 4\sqrt{\frac{2 \log(4/\delta)}{n}}. \quad (94)$$

Now, consider the reverse direction, $\hat{R}_\alpha(\theta) - R_\infty(\theta)$. We group and apply the generalization bound in addition to the inverse α -Lipschitzness (Lemma 2) to obtain

$$\begin{aligned} \hat{R}_\alpha(\theta) - R_\infty(\theta) &= \hat{R}_\infty(\theta) - R_\infty(\theta) + \hat{R}_\alpha(\theta) - \hat{R}_\infty(\theta) \\ &\leq \frac{r}{2\sqrt{n}} + 4\sqrt{\frac{2 \log(4/\delta)}{n}} + \frac{L_r}{\alpha}. \end{aligned} \quad (95)$$

Therefore, combining the two we have

$$|R_\infty(\theta) - \hat{R}_\alpha(\theta)| \leq \frac{r}{2\sqrt{n}} + 4\sqrt{\frac{2 \ln(4/\delta)}{n}} + \frac{L_r}{\alpha}, \quad (96)$$

which is the desired statement for the corollary. \square

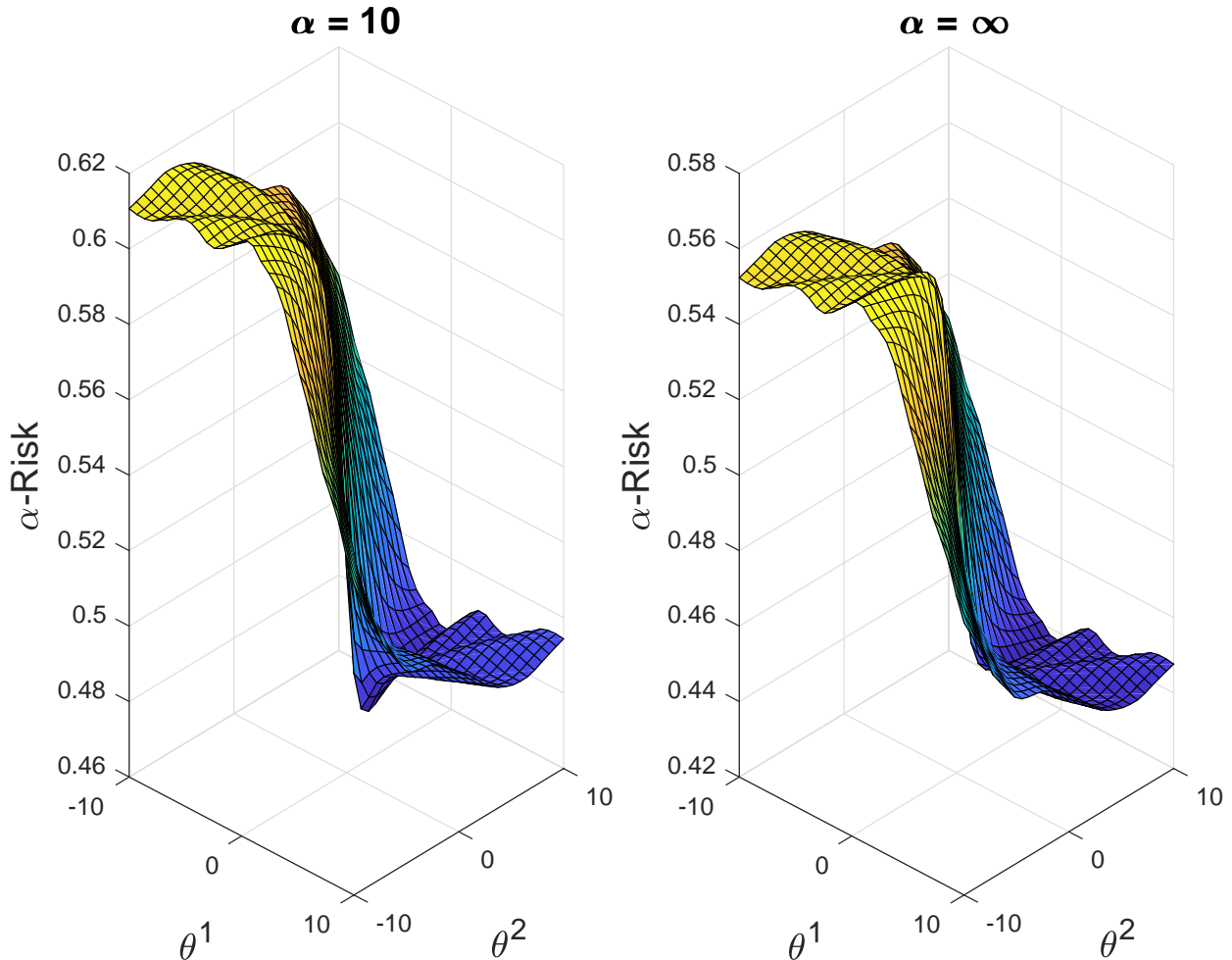


Figure 7: Saturation of α -loss (R_α for $\alpha = 10, \infty$) for a 2D-GMM under logistic regression with $\mathbb{P}[Y = 1] = \mathbb{P}[Y = -1]$, $\mu_{X|Y=-1} = [.5, .5]$, $\mu_{X|Y=1} = [1, 1]$, $\Sigma = [1, .5; .5, 3]$.

F Detailed Experimental Results

In this section, we present additional experimental results. Recall that the datasets we use are MNIST, Fashion MNIST, and CIFAR-10 all of which are largely balanced datasets, i.e., in each dataset, all ten classes are nearly equally represented. These datasets come with predefined train and test set. For the experiments, the original training set is divided into a train and validation set. The train is 90% of original training and validation is 10% of the original training set. The test set is kept the same. The neural networks chosen are described in Section 4. For all networks, we use Xavier initialization to initialize the network weights [31].

For the three types of experiments we considered, Tables 1, 2, and 4 in Section 4 summarize the accuracy results of using α -loss (in contrast to log-loss) for the original, noisy (label flipped), and (binary) imbalanced datasets, respectively. The corresponding detailed results over all datasets and architectures are presented in Tables 5, 6, and 7 here. We note that for the tables below, when using the SGD optimizer, learning rates in $[0.001, 3.0]$ were tried; for Adam we found that 0.001 worked best. Batch size of 256 is used for all experiments. Models are trained till 100 epochs and the testing epoch is chosen at the epoch at which loss of the validation set is minimized.

In addition to the three aforementioned tables, we also compare accuracies of α -loss and

log-loss when only one class of the CIFAR-10 dataset is reduced to 10% of its original size such that the imbalanced class is 1.1% of the entire dataset. We perform such comparisons for both the CNN-1 and CNN-2 architectures. These results are summarized in Table 8 where imbalances are introduced in either the auto, truck, dog, or cat classes. The results reveal significant accuracy gains in detecting the imbalanced class by tuning $\alpha < 1$.

Table 5: Accuracy (Acc.) comparison between log-loss (LL) and α -loss (α -L) for different architecture and dataset combinations using SGD or Adam. Accuracies reported are at optimal learning rates for both loss functions and accuracy maximizing (Opt.) α^* is determined over the range $[0.9 - 4]$.

Dataset	Optimizer	Architecture	LL Acc.	α -L Acc.	α^*	Rel. Gain%
MNIST	SGD	LR	0.925	0.932	2.0	0.754
		3-NN	0.981	0.981	1.2	0.038
	Adam	LR	0.927	0.934	2.0	0.735
		3-NN	0.979	0.979	0.95	0.007
Fashion MNIST	SGD	LR	0.845	0.851	4.0	0.798
		3-NN	0.889	0.891	1.7	0.213
	Adam	LR	0.847	0.853	4.0	0.657
		3-NN	0.886	0.891	1.5	0.561
CIFAR-10	SGD	LR	0.408	0.418	1.7	2.479
		3-NN	0.522	0.524	1.7	0.421
		CNN-1	0.674	0.678	1.7	0.637
	Adam	CNN-2	0.708	0.710	1.1	0.275
		CNN-1	0.675	0.674	0.9	-0.103
		CNN-2	0.724	0.729	0.95	0.648

Our experimental results also help us better understand the trade-off between accuracy and speed of convergence. We illustrate this in Figure 8 for the CIFAR-10 dataset using CNN-2. We plot the validation accuracy as a function of the number of epochs for four different values of $\alpha = \{0.95, 1, 1.5, 2.5\}$. These curves, albeit noisy, provide clear evidence of our theoretical results suggesting that the number of iterations to converge increases with α . In fact, the steep rise in accuracy of the $\alpha \leq 1$ curves relative to slower rise for $\alpha > 1$ is in line with our theoretical observations in Theorems 2 and 1 even as we recognize that with deep NNs such as CNNs used here, the landscape in general is more complex.

In Table 6, we observe that as the percentage of labels flipped increases, for a fixed architecture, α first increases and then appears to either taper off or reduce. This is indicative of the trade-off explored in Theorems 1 and 3 and Corollary 1 between robustness (and hence, better accuracy) and convergence speeds as suggested by (22) as α increases. Finally, Tables 7 and 8 highlight the significant accuracy gains resulting from exploring a range of α values. These results make a strong case for exploring the $\alpha < 1$ regime in the context of imbalanced datasets.

In particular, it is worth noting that the cat and dog classes both in the binary CIFAR and the overall CIFAR datasets are rather hard to classify well. Our results suggest significant gain in using a range of $\alpha < 1$ to enhance the classification. As the results indicate, more often than not, a small decrease in α from 1 may suffice. In particular, the result in Table 8 for the imbalanced cat class suggests one could even achieve dramatic gains (a relative gain of 108% for the cat class under CNN-1 and $\alpha^* = 0.76$) at the expense of the overall accuracy! Further exploration is needed to understand these gains better.

Table 6: Accuracy (Acc.) comparison between log-loss (LL) and α -loss (α -L) for different architecture and dataset combinations using Adam for different percentage of labels flipped. Accuracies reported are at optimal learning rates for both loss functions and accuracy maximizing (Opt.) α^* is determined over the range $[0.9 - 4]$.

Dataset	Architecture	Label Flip%	LL Acc.	α -L Acc.	α^*	Rel. Gain %
MNIST	LR	0	0.927	0.934	2.0	0.735
		5	0.920	0.934	2.5	1.457
		10	0.913	0.933	2.5	2.190
		15	0.909	0.932	4.0	2.553
		20	0.907	0.931	2.0	2.706
		25	0.901	0.930	2.5	3.256
	3-NN	0	0.979	0.979	0.95	0.007
		5	0.973	0.978	4.0	0.492
		10	0.970	0.976	3.5	0.628
		15	0.968	0.975	3.0	0.683
		20	0.966	0.973	1.5	0.680
		25	0.966	0.972	1.5	0.631
CIFAR-10	CNN-1	0	0.675	0.674	0.9	-0.103
		5	0.662	0.671	1.7	1.297
		10	0.650	0.661	1.5	1.776
		15	0.637	0.651	2.5	2.173
		20	0.627	0.650	2.0	3.576
		25	0.605	0.640	1.7	5.865
	CNN-2	0	0.724	0.729	0.95	0.648
		5	0.703	0.717	1.5	2.076
		10	0.693	0.713	1.7	2.906
		15	0.683	0.701	2.5	2.655
		20	0.672	0.696	2.0	3.477
		25	0.652	0.693	2.5	6.393

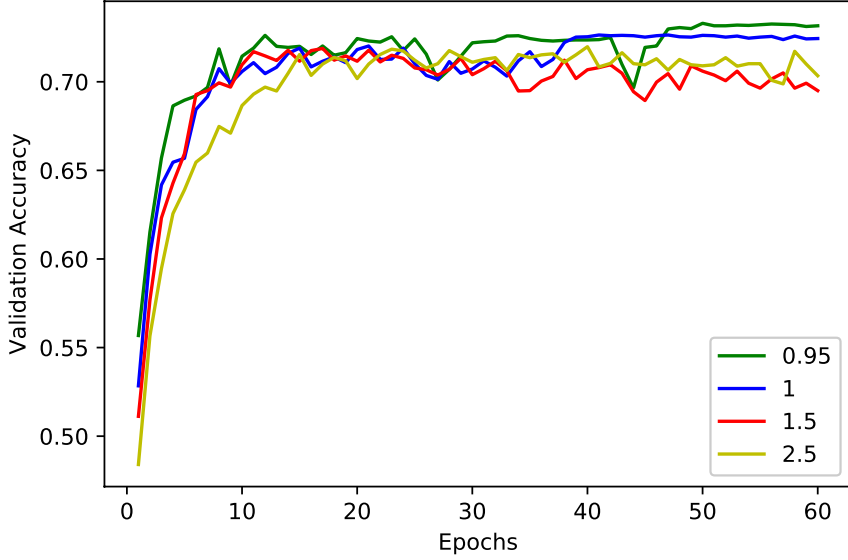


Figure 8: Validation Accuracy vs. Epochs for different Alpha

Table 7: Accuracies of less-frequent imbalanced (Imb.) class and both classes (Overall) under log-loss(LL) and α -loss(α -L) for Binary CIFAR-10 with class imbalance. Classes C1 and C2 are the dominant and less-frequent classes with 91% and 9% of all samples, respectively. Binary class pairs include {Automobile, Truck} and {Cat, Dog} from CIFAR-10 dataset.

C1	C2	Architecture	LL Acc.		α -L Acc.		Rel. Acc. Gain%		α^*
			Imb.	Overall	Imb.	Overall	Imb.	Overall	
Auto	Truck	CNN-1	0.351	0.666	0.416	0.696	18.518	4.501	0.95
		CNN-2	0.488	0.732	0.536	0.752	9.938	2.766	0.96
Truck	Auto	CNN-1	0.348	0.664	0.404	0.688	16.091	3.686	0.83
		CNN-2	0.483	0.730	0.542	0.762	12.215	4.380	1.5
Cat	Dog	CNN-1	0.111	0.549	0.174	0.573	56.756	4.458	0.9
		CNN-2	0.115	0.554	0.181	0.580	57.391	4.598	0.94
Dog	Cat	CNN-1	0.055	0.523	0.074	0.53	34.545	1.337	0.99
		CNN-2	0.122	0.554	0.143	0.560	17.622	1.173	0.74

Table 8: Accuracies of imbalanced (Imb.) class and all classes (Overall) under log-loss(LL) and α -loss(α -L) for CIFAR-10 with class imbalance. Class C is the less-frequent classes with 1.1% all samples. Less-frequent classes include Automobile (Auto.), Cat, Dog, Truck from CIFAR-10 dataset.

C	Architecture	LL Acc.		α -L Acc.		Rel. Acc. Gain%		α^*
		Imb.	Overall	Imb.	Overall	Imb.	Overall	
Auto	CNN-1	0.322	0.628	0.395	0.641	22.670	1.956	0.98
	CNN-2	0.407	0.683	0.478	0.704	17.444	3.146	0.94
Cat	CNN-1	0.049	0.652	0.102	0.645	108.163	-1.012	0.76
	CNN-2	0.089	0.701	0.119	0.707	33.707	0.826	0.93
Dog	CNN-1	0.129	0.637	0.142	0.640	10.077	0.501	0.88
	CNN-2	0.171	0.700	0.195	0.697	14.035	-0.457	0.79
Truck	CNN-1	0.269	0.631	0.344	0.632	27.881	0.205	0.93
	CNN-2	0.343	0.691	0.41	0.690	19.533	-0.115	0.73

Table 9: Accuracy (Acc.) comparison between log-loss (LL) and α -loss (α -L) for different architecture and dataset combinations using Adam for different noise levels. Accuracies reported are at optimal learning rates for both loss functions and accuracy maximizing (Opt.) α^* is determined over the range $[0.9 - 4]$. The *noise level* depicts the range $[-\text{noise level}, \text{noise level}]$ where for each selected pixel a value is drawn uniformly.

Dataset	Architecture	Noise Level	LL Acc	α -L Acc.	α^*	Rel. Gain%
MNIST	LR	25	0.922	0.928	1.7	0.642
		50	0.917	0.926	3.5	0.909
		100	0.913	0.918	2.5	0.604
		125	0.910	0.917	2.0	0.793
	3-NN	25	0.978	0.979	1.5	0.112
		50	0.977	0.977	2.0	0.033
		100	0.975	0.976	0.9	0.033
		125	0.972	0.974	1.5	0.249
CIFAR-10	CNN-1	25	0.656	0.658	1.1	0.209
		50	0.617	0.623	3.5	0.939
		100	0.537	0.540	3.0	0.529
		125	0.510	0.540	0.95	0.636
	CNN-2	25	0.713	0.712	0.95	-0.136
		50	0.687	0.689	1.1	0.159
		100	0.638	0.648	3	1.66
		125	0.610	0.627	2.5	2.839

References

- [1] P. L. Bartlett, M. I. Jordan, and J. D. McAuliffe, “Convexity, classification, and risk bounds,” *Journal of the American Statistical Association*, vol. 101, no. 473, pp. 138–156, 2006.
- [2] H. Masnadi-Shirazi and N. Vasconcelos, “On the design of loss functions for classification: theory, robustness to outliers, and SavageBoost,” in *Advances in neural information processing systems*, 2009, pp. 1049–1056.
- [3] Y. Lin, “A note on margin-based loss functions in classification,” *Statistical & Probability Letters*, vol. 68, no. 1, pp. 73–82, 2004.
- [4] L. Rosasco, E. D. Vito, A. Caponnetto, M. Piana, and A. Verri, “Are loss functions all the same?” *Neural Computation*, vol. 16, no. 5, pp. 1063–1076, 2004.
- [5] R. Nock and F. Nielsen, “On the efficient minimization of classification calibrated surrogates,” in *Advances in neural information processing systems*, 2009, pp. 1201–1208.
- [6] T. Sypherd, M. Diaz, L. Sankar, and P. Kairouz, “A tunable loss function for binary classification,” *CoRR*, vol. abs/1902.04639, 2019. [Online]. Available: <http://arxiv.org/abs/1902.04639>
- [7] J. Liao, O. Kosut, L. Sankar, and F. P. Calmon, “A tunable measure for information leakage,” in *2018 IEEE International Symposium on Information Theory (ISIT)*. IEEE, 2018, pp. 701–705.
- [8] E. Hazan, K. Levy, and S. Shalev-Shwartz, “Beyond convexity: Stochastic quasi-convex optimization,” in *Advances in Neural Information Processing Systems*, 2015, pp. 1594–1602.
- [9] X. Nguyen, M. J. Wainwright, and M. I. Jordan, “On surrogate loss functions and f -divergences,” *AOS*, vol. 37, no. 2, pp. 876–904, 04 2009.
- [10] S. Mei, Y. Bai, and A. Montanari, “The landscape of empirical risk for nonconvex losses,” *The Annals of Statistics*, vol. 46, no. 6A, pp. 2747–2774, 2018.
- [11] T. Nguyen and S. Sanner, “Algorithms for direct 0–1 loss optimization in binary classification,” in *International Conference on Machine Learning*, 2013, pp. 1085–1093.
- [12] A. Singh and J. C. Principe, “A loss function for classification based on a robust similarity metric,” in *The 2010 International Joint Conference on Neural Networks (IJCNN)*. IEEE, 2010, pp. 1–6.
- [13] A. Tewari and P. L. Bartlett, “On the consistency of multiclass classification methods,” *Journal of Machine Learning Research*, vol. 8, no. May, pp. 1007–1025, 2007.
- [14] L. Zhao, M. Mammadov, and J. Yearwood, “From convex to nonconvex: a loss function analysis for binary classification,” in *2010 IEEE International Conference on Data Mining Workshops*. IEEE, 2010, pp. 1281–1288.
- [15] K. Janocha and W. M. Czarnecki, “On loss functions for deep neural networks in classification,” *arXiv preprint arXiv:1702.05659*, 2017.
- [16] Y. E. Nesterov, “Minimization methods for nonsmooth convex and quasiconvex functions,” *Matekon*, vol. 29, pp. 519–531, 1984.
- [17] L. Benigni and S. Péché, “Eigenvalue distribution of nonlinear models of random matrices,” *arXiv preprint arXiv:1904.03090*, 2019.
- [18] L. Xiao, Y. Bahri, J. Sohl-Dickstein, S. S. Schoenholz, and J. Pennington, “Dynamical isometry and a mean field theory of cnns: How to train 10,000-layer vanilla convolutional neural networks,” *arXiv preprint arXiv:1806.05393*, 2018.
- [19] J. Pennington and P. Worah, “Nonlinear random matrix theory for deep learning,” in *Advances in Neural Information Processing Systems*, 2017, pp. 2637–2646.

- [20] J.-Y. Audibert, A. B. Tsybakov *et al.*, “Fast learning rates for plug-in classifiers,” *The Annals of statistics*, vol. 35, no. 2, pp. 608–633, 2007.
- [21] S. Arimoto, “Information measures and capacity of order α for discrete memoryless channels,” *Topics in information theory*, 1977.
- [22] Y. LeCun, C. Cortes, and C. J. C. Burges, “The MNIST database of handwritten digits,” <http://yann.lecun.com/exdb/mnist/index.html>.
- [23] H. Xiao, K. Rasul, and R. Vollgraf. (2017) Fashion-MNIST: a novel image dataset for benchmarking machine learning algorithms.
- [24] A. Krizhevsky, V. Nair, and G. Hinton, “The CIFAR-10 dataset,” *online: <http://www.cs.toronto.edu/kriz/cifar.html>*, vol. 55, 2014.
- [25] D. P. Kingma and J. Ba, “Adam: A method for stochastic optimization,” *arXiv preprint arXiv:1412.6980*, 2014.
- [26] H. Zhang, Y. Yu, J. Jiao, E. P. Xing, L. E. Ghaoui, and M. I. Jordan, “Theoretically principled trade-off between robustness and accuracy,” *arXiv preprint arXiv:1901.08573*, 2019.
- [27] A. Madry, A. Makelov, L. Schmidt, D. Tsipras, and A. Vladu, “Towards deep learning models resistant to adversarial attacks,” *arXiv preprint arXiv:1706.06083*, 2017.
- [28] L. Schmidt, S. Santurkar, D. Tsipras, K. Talwar, and A. Madry, “Adversarially robust generalization requires more data,” in *Advances in Neural Information Processing Systems*, 2018, pp. 5014–5026.
- [29] D. Yin, K. Ramchandran, and P. Bartlett, “Rademacher complexity for adversarially robust generalization,” *arXiv preprint arXiv:1810.11914*, 2018.
- [30] S. Shalev-Shwartz and S. Ben-David, *Understanding machine learning: From theory to algorithms*. Cambridge University Press, 2014.
- [31] X. Glorot and Y. Bengio, “Understanding the difficulty of training deep feedforward neural networks,” in *Proc. 13th Intl. Conf. on AI and Statistics*, Sardinia, Italy, 13–15 May 2010, pp. 249–256.
- [32] A. Raghunathan, S. M. Xie, F. Yang, J. C. Duchi, and P. Liang, “Adversarial training can hurt generalization,” *arXiv preprint arXiv:1906.06032*, 2019.
- [33] C. Huang, P. Kairouz, X. Chen, L. Sankar, and R. Rajagopal, “Context-aware generative adversarial privacy,” *Entropy*, vol. 19, no. 12, p. 656, 2017.
- [34] R. Vershynin, *High-dimensional probability: An introduction with applications in data science*. Cambridge University Press, 2018.
- [35] S. Boyd and L. Vandenberghe, *Convex optimization*. Cambridge University Press, 2004.
- [36] T. Schaul, S. Zhang, and Y. LeCun, “No more pesky learning rates,” in *International Conference on Machine Learning*, 2013, pp. 343–351.
- [37] Y. Bengio, “Practical recommendations for gradient-based training of deep architectures,” in *Neural networks: Tricks of the trade*. Springer, 2012.
- [38] W. Gao and Z.-H. Zhou, “On the consistency of multi-label learning,” in *COLT*, 2011.
- [39] O. Chapelle, C. B. Do, C. H. Teo, Q. V. Le, and A. J. Smola, “Tighter bounds for structured estimation,” in *Advances in neural information processing systems*, 2009, pp. 281–288.
- [40] Y. Wu and Y. Liu, “Robust truncated hinge loss support vector machines,” *Journal of the American Statistical Association*, vol. 102, no. 479, pp. 974–983, 2007.

- [41] A. Xu and M. Raginsky, “Information-theoretic analysis of generalization capability of learning algorithms,” in *Advances in Neural Information Processing Systems*, 2017, pp. 2524–2533.
- [42] M. Buda, A. Maki, and M. A. Mazurowski, “A systematic study of the class imbalance problem in convolutional neural networks,” *Neural Networks*, vol. 106, pp. 249 – 259, 2018. [Online]. Available: <http://www.sciencedirect.com/science/article/pii/S0893608018302107>